AJRCMB Articles in Press. Published on 11-April-2016 as 10.1165/rcmb.2016-0005OC

Knockout mice reveal a major role for alveolar epithelial type I cells in alveolar fluid clearance

Per Flodby[1*], Yong Ho Kim[1*], LaMonta L. Beard[1], Danping Gao[1], Yanbin Ji[1], Hidenori Kage[1], Janice M. Liebler[1], Parviz Minoo[2], Kwang-Jin Kim[1,3,4,5], Zea Borok[1,6**] and Edward D. Crandall[1,7,8**]

* Authors contributed equally to the manuscript
** Authors contributed equally to the manuscript

[1]Will Rogers Institute Pulmonary Research Center, Division of Pulmonary, Critical Care and Sleep Medicine, Department of Medicine, Keck School of Medicine, University of Southern California, Los Angeles, California
[2]Division of Neonatology, Department of Pediatrics, Keck School of Medicine, University of Southern California, Los Angeles, California
[3]Department of Physiology and Biophysics, Keck School of Medicine, University of Southern California, Los Angeles, California
[4]Department of Pharmacology and Pharmaceutical Sciences, School of Pharmacy, University of Southern California, Los Angeles, California
[5]Department of Biomedical Engineering, Viterbi School of Engineering, University of Southern California, Los Angeles, California
[6]Department of Biochemistry and Molecular Biology, Keck School of Medicine, University of Southern California, Los Angeles, California
[7]Department of Pathology, Keck School of Medicine, University of Southern California, Los Angeles, California
[8]Mork Family Department of Chemical Engineering and Materials Science, Viterbi School of Engineering, University of Southern California, Los Angeles, California

Correspondence and requests for reprints should be addressed to Edward D. Crandall, Ph.D., M.D., Department of Medicine, University of Southern California, IRD 620, M/C 9520, Los Angeles, California 90089-9520, USA. Phone: 323.226.7593; Fax: 323.226.2899; E-mail: ecrandal@usc.edu

Running title: Alveolar fluid clearance in *Atp1b1* knockout mice

Funding
This work was supported by the Hastings Foundation, Whittier Foundation, American Heart Association (Grant-in-Aid #12BGIA12060329 to PF) and the National Institutes of Health (R01ES017034 and U01HL108634 to EDC, R01HL056590 and R01HL095349 to PM, and R37HL062569 and R01HL112638 to ZB). P. Minoo is Hastings Professor of Pediatrics. Z. Borok is Edgington Chair in Medicine. E. D. Crandall is Hastings Professor and Norris Chair of Medicine.

Author contributions: E.D.C., Z.B. and P.M. developed concepts and approach, P.F., Y.H.K., Z.B., K.J.K. and J.M.L. conceived and designed experiments, P.F., Y.H.K., L.L.B., D.G., Y.J. and H.K. performed experiments, P.F. and Y.H.K. analyzed data, and P.F., Z.B. and E.D.C. prepared the manuscript. All authors read and approved the final manuscript.

AJRCMB Articles in Press. Published on 11-April-2016 as 10.1165/rcmb.2016-0005OC

Abstract

Active ion transport by basolateral Na-K-ATPase (Na pump) creates a Na^+ gradient that drives fluid absorption across lung alveolar epithelium. The α1 and β1 subunits are the most highly expressed Na pump subunits in alveolar epithelial cells (AEC). The specific contribution of the β1 subunit and relative contributions of alveolar epithelial type II (AT2) vs type I (AT1) cells to alveolar fluid clearance (AFC) were investigated using two cell type-specific mouse knockout lines in which β1 subunit was knocked out in either AT1 cells or in both AT1 and AT2 cells. AFC was markedly decreased in both knockout lines, revealing for the first time that AT1 cells play a major role in AFC and providing insights into AEC-specific roles in alveolar homeostasis. AEC monolayers derived from knockout mice demonstrated decreased short-circuit current and active Na^+ absorption, consistent with *in vivo* observations. Neither hyperoxia nor ventilator-induced lung injury increased wet-to-dry lung weight ratios in knockout lungs relative to controls. Knockout mice showed increases in Na pump β3 subunit expression and β_2-adrenergic receptor expression. These results demonstrate a crucial role for the Na pump β1 subunit in alveolar ion and fluid transport and indicate that both AT1 and AT2 cells make major contributions to these processes and to AFC. Furthermore, they support the feasibility of a general approach to altering alveolar epithelial function in a cell-specific manner that allows direct insights into AT1 vs AT2 cell-specific roles in the lung.

Keywords: Lung, ion transport, Na-K-ATPase, β1 subunit, β2-adrenergic receptor

AJRCMB Articles in Press. Published on 11-April-2016 as 10.1165/rcmb.2016-0005OC

Introduction

Lung alveolar epithelium, comprised of alveolar epithelial type I (AT1) and type II (AT2) cells, forms a tight barrier that limits leakage of solutes and water from the interstitial and vascular compartments into alveolar air spaces. Regulation of alveolar fluid homeostasis is based on active ion transport across the alveolar epithelium (1). Polarized localization and function of the basolateral Na-K-ATPase (Na pump) and apical sodium channels (2) are of crucial importance in transepithelial ion transport and accompanying fluid clearance across the alveolar epithelial barrier (3, 4).

AT2 cells, despite covering only about 2.5% of the alveolar surface (5), have been assumed to contribute the major portion of transport activity in alveolar epithelium based on high channel and pump density in this cell type (6). However, AT1 cells express both epithelial sodium channel (ENaC) and Na-K-ATPase subunit proteins (7-9) and, besides covering a large surface area, have very high water permeability (10). It is therefore likely that AT1 cells make an important contribution to alveolar fluid clearance (AFC) (11, 12), although the relative contributions of AT1 and AT2 cells to ion transport and AFC in the lung are entirely unknown.

The Na pump catalyzes active transport of cytoplasmic Na^+ in exchange for extracellular K^+ at the basolateral cell surface (13, 14). Na-K-ATPase is a heterotrimer comprised of one α, one β and one γ subunit. The α subunit harbors the catalytic function of the Na pump, while the β subunit is important in maturation of the structure and function of the holoenzyme and for its transport and localization to the cell membrane (15). The

function of the γ subunit is less clear, but experiments have demonstrated a modulatory role of Na pump activity and ion affinity that is tissue-specific, based on differential expression of various γ subunits (FXYD proteins) in different tissues (16). The β1 subunit is highly expressed in both AT1 and AT2 cells (17) and Na pumps comprised of α1 and β1 subunits are thought to be the predominant isozyme expressed in both cell types (18, 19), although expression of α2 subunit in lung and AT1 cells has been reported (12). A number of *in vivo* studies based on Na pump β1 subunit overexpression in rodent lungs provide evidence to support an important role of this subunit in Na pump function and AFC, both at baseline and during lung injury (19-24). Expression of the β3 subunit has been demonstrated in rat lung (25), but the role of this subunit in the lung is largely unknown. Clinically, in patients with acute lung injury/acute respiratory distress syndrome (ALI/ARDS), the capacity for higher levels of AFC is associated with better outcomes (26, 27).

The primary goals of this study were to elucidate the roles of Na pump β1 subunit in active transepithelial ion transport and AFC and to determine the relative contributions of AT1 vs AT2 cells to these processes. We generated two mouse lines with conditional knockout of the β1 subunit in either AT1 cells or in both AT1 and AT2 cells in mouse lung. This approach allows us to directly assess the contribution of the β1 subunit *in vivo* and, for the first time, to investigate specifically the roles of the two different types of alveolar epithelial cells in alveolar function. Some of the results of these studies have previously been reported in abstract form (28-30).

AJRCMB Articles in Press. Published on 11-April-2016 as 10.1165/rcmb.2016-0005OC

Materials and Methods

(See online supplement for further details.)

Generation of knockout mice

Mice with a floxed allele of the Na pump β1 subunit gene (*Atp1b1*$^{F/F}$) were generated as described in the online supplement. Briefly, *Atp1b1*$^{F/F}$ mice were crossed to *Aqp5-cre* mice (31) to generate *Atp1b1*$^{Aqp5\text{-}cre}$ mice deficient in the β1 subunit in AT1 cells, and to *Sftpc-cre* mice (32) to generate *Atp1b1*$^{Sftpc\text{-}cre}$ mice deficient in the β1 subunit in entire alveolar epithelium (i.e., both AT1 and AT2 cells). All animal protocols were approved by the Institutional Animal Care and Use Committee (IACUC) at the University of Southern California.

Alveolar fluid clearance (AFC)

Phosphate-buffered saline (PBS) with 5% bovine serum albumin (BSA, Sigma-Aldrich, St. Louis, MO) and 0.25 mg/ml BSA-Alexa Fluor 594 conjugate (Life Technologies, Carlsbad, CA) as tracer were instilled intratracheally into anesthetized mice. Alveolar fluid was aspirated after 30 minutes. AFC was calculated from fluorescence measured in instillate and aspirate.

In vivo lung permeability

Permeability *in vivo* was calculated after jugular vein injection of 10 mg fluorescein-BSA/kg body weight (Life Technologies) from fluorescence measured two hours later in bronchoalveolar lavage fluid (BALF) and serum.

Wet-to-dry lung weight ratios

Lungs were surgically removed, weighed and then dried at 65°C for 48 hours. Dry weight was recorded and wet-to-dry lung weight ratios were calculated.

Isolation of AT2 cells and primary culture of mouse alveolar epithelial cell monolayers (MAECM)

AT2 cells were isolated from mouse lungs and MAECM were cultured as previously described (33).

Bioelectric properties of MAECM

Transepithelial electrical resistance (R_T; $k\Omega \cdot cm^2$) and spontaneous potential difference (*PD*; mV) of MAECM were measured using a Millicell-ERS device (Millipore, Bedford, MA) on day 6 after AT2 cells had transdifferentiated to an AT1 cell-like phenotype. Equivalent short-circuit current (I_{EQ}; $\mu A/cm^2$) was calculated as PD/R_T. *PD* and short-circuit current (*I*sc; $\mu A/cm^2$) were measured in modified Ussing chambers in the presence or absence of terbutaline, amiloride and pimozide.

Unidirectional flux of Na^+

Unidirectional flux of Na^+ was measured across MAECM at 37°C using $^{22}NaCl$ (American Radiolabeled Chemicals, St. Louis, MO).

Western analysis

AJRCMB Articles in Press. Published on 11-April-2016 as 10.1165/rcmb.2016-0005OC

Details regarding methods and antibodies used are provided in the online supplement.

Lung histology

Standard methods as described in online supplement were used.

Antibody staining

Staining methods and antibody information are described in the online supplement.

RNA isolation, reverse transcription (RT) and quantitative polymerase chain reaction (qPCR)

Details regarding methods are provided in the online supplement. Primer sequences are shown in Table 1.

Hyperoxia exposure

Mice were housed in cages inside a hyperoxia chamber with 95% oxygen for 65 hours.

Ventilator-induced lung injury (VILI)

Anesthetized mice were ventilated with an Inspira ASV ventilator (Harvard Apparatus, Holliston, MA) under either non-injurious or injurious ventilation conditions as described in the online supplement.

Data analysis

Data are shown as mean ± SEM (standard error of the mean). Unpaired Student's *t*-test was used for comparisons of two group means. Multiple (≥3) group means were analyzed by one-way analysis of variance (ANOVA) with post-hoc tests based on Student-Newman-Keuls approaches. P <0.05 is considered statistically significant.

Results

Atp1b1 gene targeting and generation/verification of β1 knockout mice

We generated a mouse line with a conditional (floxed) allele of the *Atp1b1* gene (encoding the Na-K-ATPase β1 subunit) to enable cell-specific gene knockout by Cre/loxP recombination (Figure 1). Mouse *Atp1b1* contains six exons, where exon 1 codes for the cytoplasmic domain of the Na-K-ATPase β1 subunit protein and the first part of exon 2 codes for the transmembrane domain. The remainder of the gene codes for the large extracellular domain which makes up 243 of the 305 amino acids in this protein. We flanked exon 4 of *Atp1b1* with loxP sites in order to create a conditional allele of this gene ($Atp1b1^{F/F}$, Figure 1). Cre/loxP-mediated deletion of exon 4 results in a frame-shift mutation after splicing of exon 3 to exon 5. To elucidate the importance of the β1 subunit in adult mouse lung fluid homeostasis and its relative importance in AT1 versus AT2 cells, we generated two separate lines, one harboring a conditional β1 knockout specifically in AT1 cells using *Aqp5-cre* mice (31) and one in which β1 was inactivated in both AT1 and AT2 cells (alveolar epithelium-specific knockout) using *Sftpc-cre* mice (32). These two knockout lines are referred to as $Atp1b1^{Aqp5\text{-}cre}$ and $Atp1b1^{Sftpc\text{-}cre}$, respectively. Knockout lines were analyzed in order to verify deletion of

AJRCMB Articles in Press. Published on 11-April-2016 as 10.1165/rcmb.2016-0005OC

the Na pump β1 subunit gene (see online supplement). Genomic PCR (Supplementary Figure E1A) confirmed that the floxed *Atp1b1* allele could be correctly deleted by Cre/loxP recombination. Western analysis (Supplementary Figure E1B) confirmed that Na pump β1 protein was absent in AT2 cells isolated from $Atp1b1^{Sftpc\text{-}cre}$ knockout mice. We confirmed (Supplementary Figure E1C) that *Aqp5-cre* activates green fluorescent protein (GFP) expression from a $ROSA^{mT/mG}$ reporter transgene specifically in AT1 cells in the alveolar epithelium and that efficiency of this Cre/loxP mediated reporter activation is very high (>90% of AT1 cells) (31). Finally, we confirmed that *Sftpc-cre* activates GFP expression in the $ROSA^{mT/mG}$ reporter transgene in both AT1 and AT2 cells, although the GFP signal is considerably stronger in AT2 cells, in part reflecting the very thin AT1 cell architecture *in vivo* (Supplementary Figure E1C).

AFC is markedly reduced in mice deficient in the Na pump β1 subunit

We measured AFC in the two β1 subunit knockout lines ($Atp1b1^{Aqp5\text{-}cre}$ and $Atp1b1^{Sftpc\text{-}cre}$) and compared them to respective floxed litter mate control mice ($Atp1b1^{F/F}$). AFC in $Atp1b1^{Aqp5\text{-}cre}$ knockout mice, deficient in the β1 subunit specifically in AT1 cells, demonstrated a highly significant (P = 0.006) reduction (43%) in AFC compared to $Atp1b1^{F/F}$ controls (Figure 2A). $Atp1b1^{Sftpc\text{-}cre}$ knockouts, which lack the β1 subunit in both AT1 and AT2 cells, revealed even lower AFC, which was significantly (P = 0.002) reduced by 78% compared to controls (Figure 2B). These data demonstrate that the Na pump β1 subunit is of crucial importance in AFC following fluid instillation and that both AT1 and AT2 cells make major contributions to AFC in the adult mouse lung. The portion of AFC attributable to AT1 and AT2 cells can be estimated as ~55% (i.e.,

43/78=0.55) and ~45% (i.e., (78-43)/78=0.45), respectively, assuming that AT1/AT2 cell number ratios are similar in control and knockout mice based on histological examination of lungs from floxed controls and both knockout lines that showed no obvious morphologic differences (Supplementary Figure E2). AFC in *Atp1b1*$^{Aqp5\text{-}cre}$ and *Atp1b1*$^{Sftpc\text{-}cre}$ knockout mice (57% and 22%, respectively, relative to floxed controls) are likely based on active sodium transport due to residual Na pump activity.

Unchanged lung permeability and absence of lung edema in β1 knockouts

To investigate if β1 knockout lungs have altered paracellular permeability that might contribute to reductions in AFC, we injected fluorescein-bovine serum albumin (BSA) into the jugular vein of floxed and knockout mice. As shown in Figures 2C and 2D, lung permeability to fluorescein-BSA was not different in β1 knockout mice compared to floxed controls. Consistent with these findings, lungs of both *Atp1b1*$^{Aqp5\text{-}cre}$ and *Atp1b1*$^{Sftpc\text{-}cre}$ mice had wet-to-dry lung weight ratios that were not different from their respective floxed controls (Figures 2E and 2F), suggesting that, in both β1 subunit knockout lines, residual Na pump activity is sufficient to maintain lung fluid homeostasis.

Decreased I_{EQ} and unchanged R_T across MAECM deficient in β1 subunit

Bioelectric properties (transepithelial electrical resistance R_T and equivalent short-circuit current I_{EQ}) were evaluated in mouse alveolar epithelial cell monolayers (MAECM) prepared by cultivation of freshly isolated AT2 cells derived from *Atp1b1*$^{F/F}$ control and *Atp1b1*$^{Sftpc\text{-}cre}$ knockout mice. As shown in Figure 3A, R_T of *Atp1b1*$^{F/F}$ control and *Atp1b1*$^{Sftpc\text{-}cre}$ knockout monolayers on day 6 were not significantly different. In contrast,

AJRCMB Articles in Press. Published on 11-April-2016 as 10.1165/rcmb.2016-0005OC

I_{EQ} of *Atp1b1*$^{Sftpc\text{-}cre}$ knockout monolayers was significantly reduced compared to *Atp1b1*$^{F/F}$ control monolayers, consistent with results *in vivo* (Figure 3B) and supporting the observation that the Na pump β1 subunit plays a crucial role in active ion transport across MAECM.

Decreased Na^+ absorption in MAECM deficient in β1 subunit

In order to more directly evaluate active ion transport across *Atp1b1*$^{F/F}$ control and *Atp1b1*$^{Sftpc\text{-}cre}$ knockout MAECM, unidirectional Na^+ flux and net Na^+ absorption were determined under zero electrical gradient (i.e., short-circuit) conditions in Ussing chambers. Figure 3C shows the unidirectional Na^+ flux in each direction (i.e., apical-to-basolateral (A→B) and basolateral-to-apical (B→A)). In both control and knockout monolayers, unidirectional Na^+ flux in the A→B direction was significantly greater than that in the B→A direction. Knockout monolayers had significantly lower unidirectional Na^+ flux in the A→B direction (P <0.01), and unchanged unidirectional Na^+ flux in the B→A direction, compared to control monolayers. Baseline net Na^+ absorption of knockout monolayers was significantly lower than that of control monolayers (Figure 3D). Net Na^+ absorption in control and knockout monolayers was not significantly different from the observed active ion transport rate (i.e., short-circuit current I_{SC}) during the Na^+ flux measurements (data not shown), indicating that estimated net Na^+ absorption accounts for most of the observed active ion transport across MAECM.

Sodium channel function unaffected by β1 knockout

Alveolar epithelial cells harbor apical amiloride-sensitive sodium channels (ENaC) and pimozide-sensitive cyclic nucleotide-gated (CNG) nonselective cation channels (4). In order to determine if knockout of the Na pump β1 subunit had any effects on these ion channels, MAECM were treated with ENaC or CNG channel inhibitors and bioelectrical properties were evaluated. Addition of amiloride to apical fluid caused a rapid ~70% decrease in I_{SC} of both control and knockout MAECM (Figures 4A and 4B). Subsequent treatment with apical pimozide at 60 minutes led to a slight additional decrease in I_{SC} of both monolayers. When the CNG inhibitor pimozide was added first, I_{SC} of both control and knockout monolayers gradually decreased by ~45% (Figures 4C and 4D). When amiloride (10 μM) was subsequently added to apical fluid, I_{SC} of both monolayers rapidly decreased further by ~35%. These data suggest that the function of apical sodium channels remains unchanged in β1 knockout MAECM.

Wet-to-dry lung weight ratios after hyperoxia or ventilator-induced lung injury (VILI)

Although residual AFC in both β1 knockout lines was sufficient to maintain normal lung fluid balance in the unchallenged lung, we assessed whether or not decreased AFC in mice deficient in the β1 subunit affected their susceptibility to lung injury from hyperoxia or VILI. All animals developed increased wet-to-dry lung weight ratios after exposure to >95% oxygen for 65 hours (Figure 5A), but neither $Atp1b1^{Aqp5\text{-}cre}$ nor $Atp1b1^{Sftpc\text{-}cre}$ knockout mice exhibited ratios different from $Atp1b1^{F/F}$ control mice subjected to the same experimental conditions. Mice of both $Atp1b1^{F/F}$ and $Atp1b1^{Sftpc\text{-}cre}$ genotypes mechanically ventilated for 3 hours with a peak inspiratory pressure (PIP) of 40 cmH_2O and without positive-end expiratory pressure (PEEP) had significantly higher wet-to-dry

AJRCMB Articles in Press. Published on 11-April-2016 as 10.1165/rcmb.2016-0005OC

lung weight ratios compared to mice ventilated under non-injurious conditions at 20 cmH_2O, also without PEEP (Figure 5B), but there was no significant difference in wet-to-dry weight ratios between controls and knockouts after VILI.

Increased expression of Na pump β3 subunit protein in Atp1b1$^{Sftpc\text{-}cre}$ knockout mice

Both *Atp1b1$^{Aqp5\text{-}cre}$* and *Atp1b1$^{Sftpc\text{-}cre}$* knockout mice had normal wet-to-dry lung weight ratios at baseline (Figures 2E and F), suggesting that residual Na-K-ATPase activity was sufficient to maintain fluid homeostasis. The Na pump β3 subunit is the second highest expressed β subunit in alveolar epithelial cells. Western analysis revealed increased β3 protein expression in freshly isolated AT2 cells derived from *Atp1b1$^{Sftpc\text{-}cre}$* mice (Figures 6A and B), and antibody staining of MAECM from knockout mice showed increased expression of β3 subunit protein compared to control MAECM (Figures 6C and D), although β3 subunit expression at the mRNA level in whole lung, freshly isolated AT2 cells or MAECM did not change (Figures 6E-H). Relative mRNA expression levels of other α and β subunit genes in whole lung of *Atp1b1$^{Aqp5\text{-}cre}$* knockout mice were either unchanged or only moderately different from *Atp1b1$^{F/F}$* control lungs, while in *Atp1b1$^{Sftpc\text{-}cre}$* knockout lungs a more substantial reduction in β1 subunit RNA levels was observed (Figure 6F), likely due to the fact that the β1 gene is deleted in the entire epithelium. Similarly, *Atp1b1$^{Sftpc\text{-}cre}$* knockout AT2 cells and MAECM demonstrated significantly lower expression of β1 subunit (Figures 6G and H). Expression of Na pump α1 subunit protein in AT2 cells obtained from *Atp1b1$^{Sftpc\text{-}cre}$* knockout mice was unchanged, while β1 subunit protein was absent (Figure 6A).

Increased expression of β3 subunit protein may contribute to residual AFC in *Atp1b1*$^{Sftpc\text{-}cre}$ knockout mice.

Increased β_2-adrenergic responsiveness in vivo in β1 subunit knockouts

When terbutaline was added to the fluid instillate in AFC experiments, AFC increased markedly in both *Atp1b1*$^{Aqp5\text{-}cre}$ and *Atp1b1*$^{Sftpc\text{-}cre}$ knockout mice, reaching levels close to those measured in *Atp1b1*$^{F/F}$ control mice (+Terbutaline in Figures 7A and B). This was in contrast to AFC in the absence of terbutaline, which showed significantly lower AFC in both knockouts (-Terbutaline in Figures 7A and B). To investigate the possibility that these observations could be due to higher expression of the β_2-adrenergic receptor (β_2AR) in knockout mice, we performed Western analysis on whole lung. As shown in Figure 7C and D, β_2AR protein levels were significantly higher in the lungs of mice from both knockout lines compared to controls, which may contribute to increased responsiveness to terbutaline stimulation and residual AFC in *Atp1b1*$^{Aqp5\text{-}cre}$ and *Atp1b1*$^{Sftpc\text{-}cre}$ knockout mice.

Discussion

We generated and analyzed two mouse lines harboring knockouts of the Na-K-ATPase β1 subunit, either in AT1 cells only (*Atp1b1*$^{Aqp5\text{-}cre}$ mice) or in both AT1 and AT2 cells (*Atp1b1*$^{Sftpc\text{-}cre}$ mice) in the lung. AFC was reduced by 78% in *Atp1b1*$^{Sftpc\text{-}cre}$ mice, providing evidence for an important role of the β1 subunit under conditions of excess alveolar fluid volume. AFC was also substantially reduced in *Atp1b1*$^{Aqp5\text{-}cre}$ mice (by 43%), indicating that AT1 cells are major contributors to active ion transport and

AJRCMB Articles in Press. Published on 11-April-2016 as 10.1165/rcmb.2016-0005OC

associated fluid clearance (~55% of overall AFC) in mouse lung. There were no changes in lung permeability in mice deficient in the Na pump β1 subunit. Despite lower active ion transport and decreased AFC, both knockout lines had normal wet-to-dry lung weight ratios at baseline, and no differences in wet-to-dry lung weight ratios were observed among genotypes after hyperoxia or VILI. Analysis of bioelectric properties of cultured AEC monolayers demonstrated that AT1-like cells deficient in the Na pump β1 subunit featured significantly decreased active Na^+ absorption and I_{EQ} (and I_{SC}), consistent with the observation that knockout mice were unable to clear fluid at the same rate as floxed control mice and demonstrating that the β1 subunit is crucial to AFC. Finally, *in vitro* analysis revealed that R_T was unaffected in MAECM deficient in the β1 subunit, consistent with unchanged permeability in knockout lung.

Cell-specific deletion of Atp1b1 and effects on Na pump subunit expression

In Figure 6E, which shows subunit expression levels in whole lung in AT1 cell-specific knockouts, the decrease in β1 mRNA did not reach statistical significance. Given the fact that AT2 cells are present in larger numbers than AT1 cells in the lung (~2:1) (5), a relatively limited effect on whole lung β1 expression levels might be expected in AT1 cell-specific knockout lungs. It is also possible that the β1 expression level per cell differs between wildtype AT1 vs AT2 cells. If the level is higher in AT2 cells, this would also contribute to the apparent limited decrease in β1 mRNA in whole lungs of AT1 cell-specific knockouts. A compensatory increase in β1 expression in AT2 cells in AT1 cell-specific knockouts would have the same effect of masking the decreased mRNA level in AT1 cells when analyzing expression in whole lung. The decreased mRNA levels of α1,

α2 and β2 subunits in freshly isolated AT2 cells shown in Figure 6G were relatively small but nevertheless significant. At the protein level, we were able to detect α1, which did not change significantly (Figure 6A), while α2 and β2 proteins were undetectable. From other studies involving sodium pump subunits, it is known that changes in mRNA level are not always reflected at the protein level (e.g., β1 subunit is increased at the mRNA level in rat lung exposed to hyperoxia, while no corresponding increase in β1 protein was found (34)).

Relative contributions of AT1 and AT2 cells to alveolar ion and water transport

AT1 cell-specific β1 knockout mice showed ~43% reduction in AFC, while animals lacking β1 in both AT1 and AT2 cells demonstrated ~78% reduction in AFC. As noted above, these results indicate that a major portion (~55%) of AFC in the lung is normally driven by AT1 cells, providing the first direct evidence to support a major contribution of AT1 cells to AFC in the lung. Considering that the number of AT2 cells in the lung is greater than that of AT1 cells (5), AFC contributed per AT1 cell is greater than that per AT2 cell. This finding contrasts with the earlier presumption that AT2 cells are responsible for most of the ion (and accompanying fluid) transport in the lung (6). However, since total surface area of AT1 cells is much larger than that of AT2 cells (73-fold difference in rat lung (5)), the density of Na pumps per AT2 cell is likely much higher than that per AT1 cell. In these calculations of relative contribution to AFC from AT1 and AT2 cells, we assumed that β1 is efficiently and similarly knocked out in both AT2 and AT1 cells in the *Atp1b1*$^{Sftpc\text{-}cre}$ knockout line, which is likely since the *Sftpc* promoter driving the *cre* transgene starts to be expressed very early during lung

AJRCMB Articles in Press. Published on 11-April-2016 as 10.1165/rcmb.2016-0005OC

development (35) and the *Atp1b1* gene will thus be deleted in progenitors of both AT2 and AT1 cells (36). Figure E1C (right panel) shows efficient Cre-mediated reporter activation, resulting in GFP expression in both AT1 and AT2 cells, although expression is considerably weaker in AT1 cells. Since the mGFP reporter protein (myristoylated GFP) encoded by the $ROSA^{mT/mG}$ transgene is inserted into the plasma membrane, an equal amount of mGFP expressed per cell in AT2 and AT1 cells would be expected to result in a weaker signal in AT1 cells given their considerably larger cell surface area. When comparing the two knockout lines and calculating relative contributions of AT1 and AT2 cells, we have assumed equal knockout efficiency in AT1 cells in the two lines based on efficient reporter activation in AT1 cells in both $Aqp5^{cre};ROSA^{mT/mG}$ and $Sftpc^{cre};ROSA^{mT/mG}$ (as shown in Figure E1C, left and right panel, respectively).

Changes in transport properties of β1 knockout MAECM

Isolated mouse AT2 cells cultured on polycarbonate filters transdifferentiate into AT1-like cells, forming functional monolayers with high R_T that are suitable for characterization of ion transport and bioelectric properties (33). Given that Na pump β1 subunit is the most highly expressed β subunit in lung, we hypothesized that knockout of *Atp1b1* would result in decreased active Na^+ transport. MAECM deficient in β1 subunit exhibited lower net Na^+ absorption compared to MAECM from floxed mice. These results demonstrating the importance of Na pump β1 subunit for ion transport in AT1-like cells in culture are consistent with our findings *in vivo* in $Atp1b1^{Aqp5\text{-}cre}$ mice in which deletion of β1 specifically in AT1 cells resulted in a major reduction in AFC. In experiments to evaluate responses in MAECM to an inhibitor of ENaC (amiloride) and

CNG (pimozide) channels, we found proportional inhibition of active ion transport in knockout and control mice, suggesting that β1 subunit deficiency does not alter relative contributions of these channels to transepithelial ion transport. However, as pimozide is known to affect D_2-dopamine receptors, we cannot completely rule out the possibility that the observed pimozide effects on I_{SC} might have been different between the genotypes. Increased expression of β3 subunit and β_2AR in MAECM were not sufficient to restore ion transport. Although β1 subunits in neighboring cells have been reported to interact directly as adhesion molecules (37-39), R_T was not decreased in β1 knockout MAECM. Although not included in this study, evaluation of bioelectric properties of MAECM derived from AT2 cells of *Atp1b1*$^{Aqp5\text{-}cre}$ mice would show the effects of *de novo* β1 gene deletion. Thus, the β1 subunit gene would be gradually deleted during the process of AT2 cell transdifferentiation into AT1 cells, since transdifferentiated cells start to express *Aqp5* and Cre. In both knockout models, deletion of the β1 subunit gene is dependent on the spatiotemporal expression profile of the promoter driving Cre expression. *Sftpc-cre* is expressed already in early lung progenitors in the developing embryo, while *Aqp5-cre* reaches appreciable expression levels perinatally. Since all studies were performed in adult mice, compensatory mechanisms may have developed in both knockout lines.

Response to lung injury in β1 knockout mice

We did not detect any differences in wet-to-dry lung weight ratios among genotypes after hyperoxia or VILI, although wet-to-dry lung weight ratios are relatively insensitive to small changes in alveolar fluid volume. While AFC data would have been more

AJRCMB Articles in Press. Published on 11-April-2016 as 10.1165/rcmb.2016-0005OC

useful, technical challenges prevented accurate measurement of AFC in injured lungs. The absence of higher wet-to-dry lung weight ratios after injury in β1 knockout mice vs controls might be due in part to a compensatory increase in expression of sodium pump β3 subunit and/or elevated expression of β2 adrenergic receptors. Expression of β3 subunit has been reported in normal rat lungs (25), but there have been no reports on its role in lung injury. Elevated expression of β2 adrenergic receptors in knockout mice correlated with increased responsiveness to terbutaline, supporting a potential role of adrenergic signaling as a compensatory mechanism in β1 knockout lungs. A higher increase (~4-fold) in AFC in response to terbutaline in *Atp1b1*$^{Sftpc\text{-}cre}$ knockouts is likely a reflection of increased adrenergic signaling in both AT1 and AT2 cells, since both cell types lack β1 in this knockout line. In *Atp1b1*$^{Aqp5\text{-}cre}$ knockouts, however, β1 is missing only in AT1 cells, so the adrenergic response will be less pronounced (~2-fold) since increased adrenergic signaling likely only takes place in AT1 cells. This reasoning is based on the assumption that increased adrenergic signaling is an intrinsic response in cells lacking the β1 protein and that increased adrenergic responsiveness is only found in these cells. We did not investigate expression levels of Na pump γ subunits in β1 knockout mice, although a recent report demonstrated expression of all seven FXYD genes (encoding γ subunits) in human lung at the mRNA level (40). This study also suggested that FXYD1 is a negative regulator of Na pump activity and that increased expression of FXYD1 in lungs from patients with ARDS may indicate a role for γ subunits in deficient ion transport and fluid clearance.

Summary

These findings from lung epithelial cell type-specific β1 subunit knockout mice demonstrate a major contribution of AT1 cells, greater than that of AT2 cells, to alveolar ion transport and AFC. Residual AFC in β1 subunit knockout mice, possibly due in part to increased expression of β3 subunit and β_2-adrenergic receptors, appears sufficient to maintain lung fluid homeostasis at baseline. These studies demonstrate for the first time that the roles of lung alveolar epithelial cells can be addressed in an AT1 vs AT2 cell-specific manner *in vivo*, leading to improved understanding of clinical implications pertaining to specific cell types in alveolar epithelium. Elucidation of the relative contributions of AT1 and AT2 cells to alveolar function/homeostasis may help lead to development of new therapeutic approaches to lung disease.

Acknowledgements

We thank the USC Transgenic Core under the direction of Dr. Robert Maxson and Dr. Nancy Wu for fruitful collaborations to establish *Atp1b1*$^{F/F}$ mice, Dr. Gökhan Mutlu, Northwestern University, for generously sharing mouse AFC protocols and expertise, and Dr. Alicia McDonough, USC, for sharing rabbit polyclonal β3 antibodies. Histology and microscopy services were provided by the Cell and Tissue Imaging Core of the USC Research Center for Liver Diseases (NIH P30 DK048522 and S10 RR022508).

AJRCMB Articles in Press. Published on 11-April-2016 as 10.1165/rcmb.2016-0005OC

References

1. Matthay MA, Clerici C, Saumon G. Active fluid clearance from the distal air spaces of the lung. *J Appl Physiol* 2002; 93: 1533-1541.

2. Hummler E, Planes C. Importance of ENaC-mediated sodium transport in alveolar fluid clearance using genetically-engineered mice. *Cell Physiol Biochem* 2010; 25: 63-70.

3. Norlin A, Lu LN, Guggino SE, Matthay MA, Folkesson HG. Contribution of amiloride-insensitive pathways to alveolar fluid clearance in adult rats. *J Appl Physiol* 2001; 90: 1489-1496.

4. Wilkinson W, Benjamin A, De Proost I, Orogo-Wenn M, Yamazaki Y, Staub O, Morita T, Adriaensen D, Riccardi D, Walters D, Kemp P. Alveolar epithelial CNGA1 channels mediate cGMP-stimulated, amiloride-insensitive, lung liquid absorption. *Pflügers Archiv - Europ J Physiol* 2011; 462: 267-279.

5. Haies DM, Gil J, Weibel ER. Morphometric study of rat lung cells. I. Numerical and dimensional characteristics of parenchymal cell population. *Am Rev Respir Dis* 1981; 123: 533-541.

6. Schneeberger EE, McCarthy KM. Cytochemical localization of Na^+-K^+-ATPase in rat type II pneumocytes. *J Appl Physiol* 1986; 60: 1584-1589.

7. Borok Z, Liebler JM, Lubman RL, Foster MJ, Zhou B, Li X, Zabski SM, Kim KJ, Crandall ED. Na transport proteins are expressed by rat alveolar epithelial type I cells. *Am J Physiol Lung Cell Mol Physiol* 2002; 282: L599-L608.

8. Johnson MD, Widdicombe JH, Allen L, Barbry P, Dobbs LG. Alveolar epithelial type I cells contain transport proteins and transport sodium, supporting an active role

for type I cells in regulation of lung liquid homeostasis. *Proc Natl Acad Sci U S A* 2002; 99: 1966-1971.

9. Crandall ED, Matthay MA. Alveolar epithelial transport. Basic science to clinical medicine. *Am J Respir Crit Care Med* 2001; 163: 1021-1029.
10. Dobbs LG, Gonzalez R, Matthay MA, Carter EP, Allen L, Verkman AS. Highly water-permeable type I alveolar epithelial cells confer high water permeability between the airspace and vasculature in rat lung. *Proc Natl Acad Sci U S A* 1998; 95: 2991-2996.
11. Johnson MD, Bao HF, Helms MN, Chen XJ, Tigue Z, Jain L, Dobbs LG, Eaton DC. Functional ion channels in pulmonary alveolar type I cells support a role for type I cells in lung ion transport. *Proc Natl Acad Sci U S A* 2006; 103: 4964-4969.
12. Ridge KM, Olivera WG, Saldias F, Azzam Z, Horowitz S, Rutschman DH, Dumasius V, Factor P, Sznajder JI. Alveolar type 1 cells express the α2 Na,K-ATPase, which contributes to lung liquid clearance. *Circ Res* 2003; 92: 453-460.
13. Rajasekaran SA, Rajasekaran AK. Na,K-ATPase and epithelial tight junctions. *Front Biosci* 2009; 14: 2130-2148.
14. Kaplan JH. Biochemistry of Na,K-ATPase. *Ann Rev Biochem* 2002; 71: 511-535.
15. Geering K, Theulaz I, Verrey F, Hauptle MT, Rossier BC. A role for the β-subunit in the expression of functional Na^+-K^+-ATPase in Xenopus oocytes. *Am J Physiol Cell Physiol* 1989; 257: C851-C858.
16. Geering K. Functional roles of Na,K-ATPase subunits. *Curr Opin Nephrol Hypertens* 2008; 17: 526-532.

AJRCMB Articles in Press. Published on 11-April-2016 as 10.1165/rcmb.2016-0005OC

17. Zhang XL, Danto SI, Borok Z, Eber JT, Martin-Vasallo P, Lubman RL. Identification of Na^+-K^+-ATPase β-subunit in alveolar epithelial cells. *Am J Physiol* 1997; 272: L85-L94.

18. Borok Z, Danto SI, Dimen LL, Zhang XL, Lubman RL. Na^+-K^+-ATPase expression in alveolar epithelial cells: upregulation of active ion transport by KGF. *Am J Physiol* 1998; 274: L149-L158.

19. Factor P, Saldias F, Ridge K, Dumasius V, Zabner J, Jaffe HA, Blanco G, Barnard M, Mercer R, Perrin R, Sznajder JI. Augmentation of lung liquid clearance via adenovirus-mediated transfer of a Na,K-ATPase β1 subunit gene. *J Clin Invest* 1998; 102: 1421-1430.

20. Machado-Aranda D, Adir Y, Young JL, Briva A, Budinger GRS, Yeldandi AV, Sznajder JI, Dean DA. Gene transfer of the Na^+,K^+-ATPase β1 subunit using electroporation increases lung liquid clearance. *Am J Respir Crit Care Med* 2005; 171: 204-211.

21. Factor P, Dumasius V, Saldias F, Brown LA, Sznajder JI. Adenovirus-mediated transfer of an Na^+/K^+-ATPase β1 subunit gene improves alveolar fluid clearance and survival in hyperoxic rats. *Hum Gene Ther* 2000; 11: 2231-2242.

22. Azzam ZS, Dumasius V, Saldias FJ, Adir Y, Sznajder JI, Factor P. Na,K-ATPase overexpression improves alveolar fluid clearance in a rat model of elevated left atrial pressure. *Circulation* 2002; 105: 497-501.

23. Adir Y, Factor P, Dumasius V, Ridge KM, Sznajder JI. Na,K-ATPase gene transfer increases liquid clearance during ventilation-induced lung injury. *Am J Respir Crit Care Med* 2003; 168: 1445-1448.

24. Mutlu GM, Machado-Aranda D, Norton JE, Bellmeyer A, Urich D, Zhou R, Dean DA. Electroporation-mediated gene transfer of the Na^+,K^+-ATPase rescues endotoxin-induced lung injury. *Am J Respir Crit Care Med* 2007; 176: 582-590.

25. Arystarkhova E, Sweadner KJ. Tissue-specific expression of the Na,K-ATPase β3 subunit. *J Biol Chem* 1997; 272: 22405-22408.

26. Ware LB, Matthay MA. Alveolar fluid clearance is impaired in the majority of patients with acute lung injury and the acute respiratory distress syndrome. *Am J Respir Crit Care Med* 2001; 163: 1376-1383.

27. Sznajder JI. Alveolar edema must be cleared for the acute respiratory distress syndrome patient to survive. *Am J Respir Crit Care Med* 2001; 163: 1293-1294.

28. Flodby P, Borok Z, Kim YH, Banfalvi A, Kim KJ, Crandall ED. AT1 cell-specific knockout of the sodium pump β1 subunit gene (Atp1b1) results in impaired alveolar fluid clearance. *Am J Respir Crit Care Med* 2011; 183: A4230 (Abstract).

29. Kim YH, Flodby P, DeMaio L, Kim KJ, Crandall ED, Borok Z. Decreased active ion transport across primary cultured alveolar epithelial cell monolayers generated from Na+,K+-ATPase β1-subunit knockout mice. *Am J Respir Crit Care Med* 2011; 183: A4231 (Abstract).

30. Flodby P, Borok Z, Gao D, Kim YH, Kim KJ, Crandall ED. Role of sodium pump β1 subunit in adult mouse lung alveolar fluid homeostasis. *FASEB J* 2012; 26: 1069.1066 (Abstract).

31. Flodby P, Borok Z, Banfalvi A, Zhou B, Gao D, Minoo P, Ann DK, Morrisey EE, Crandall ED. Directed expression of Cre in alveolar epithelial type 1 cells. *Am J Respir Cell Mol Biol* 2010; 43: 173-178.

AJRCMB Articles in Press. Published on 11-April-2016 as 10.1165/rcmb.2016-0005OC

32. Okubo T, Knoepfler PS, Eisenman RN, Hogan BL. Nmyc plays an essential role during lung development as a dosage-sensitive regulator of progenitor cell proliferation and differentiation. *Development* 2005; 132: 1363-1374.

33. DeMaio L, Tseng W, Balverde Z, Alvarez JR, Kim KJ, Kelley DG, Senior RM, Crandall ED, Borok Z. Characterization of mouse alveolar epithelial cell monolayers. *Am J Physiol Lung Cell Mol Physiol* 2009; 296: L1051-L1058.

34. Carter EP, Wangensteen OD, O'Grady SM, Ingbar DH. Effects of hyperoxia on type II cell Na-K-ATPase function and expression. *Am J Physiol* 1997; 272: L542-551.

35. Wert SE, Glasser SW, Korfhagen TR, Whitsett JA. Transcriptional elements from the human SP-C gene direct expression in the primordial respiratory epithelium of transgenic mice. *Dev Biol* 1993; 156: 426-443.

36. Desai TJ, Brownfield DG, Krasnow MA. Alveolar progenitor and stem cells in lung development, renewal and cancer. *Nature* 2014; 507: 190-194.

37. Shoshani L, Contreras RG, Roldan ML, Moreno J, Lazaro A, Balda MS, Matter K, Cereijido M. The polarized expression of Na^+,K^+-ATPase in epithelia depends on the association between β-subunits located in neighboring cells. *Mol Biol Cell* 2005; 16: 1071-1081.

38. Vagin O, Tokhtaeva E, Sachs G. The role of the β1 subunit of the Na,K-ATPase and its glycosylation in cell-cell adhesion. *J Biol Chem* 2006; 281: 39573-39587.

39. Vagin O, Dada LA, Tokhtaeva E, Sachs G. The Na-K-ATPase $\alpha 1\beta 1$ heterodimer as a cell adhesion molecule in epithelia. *Am J Physiol Cell Physiol* 2012; 302: C1271-C1281.

40. Wujak LA, Blume A, Baloglu E, Wygrecka M, Wygowski J, Herold S, Mayer K, Vadasz I, Besuch P, Mairbaurl H, Seeger W, Morty RE. FXYD1 negatively regulates Na(+)/K(+)-ATPase activity in lung alveolar epithelial cells. *Respir Physiol Neurobiol* 2016; 220: 54-61.

AJRCMB Articles in Press. Published on 11-April-2016 as 10.1165/rcmb.2016-0005OC

Table 1. qRT-PCR primers

Gene	GenBank Accession No.	Primer Sequence (5' → 3')	Product Size (bp)
Atp1a1 (Na^+,K^+-ATPase α1)	NM_144900	TCAAGTCTTGGAGCTCGGAACT (FP) ACGTCTGCATCCCCACATG (RP)	66
Atp1a2 (Na^+,K^+-ATPase α2)	NM_178405	TGAGCTGGGCCGAAAATACC (FP) GGGTCCATCTCTAGCCAGAAT (RP)	85
Atp1a3 (Na^+,K^+-ATPase α3)	BC034645	TCTGCCCTGCTTAAGTGCATT (FP) TCCGTTCTCGCATCAGCTT (RP)	61
Atp1a4 (Na^+,K^+-ATPase α4)	NM_013734	TCAGGAGTCTGTTCCCATAGCTAA (FP) GGAGAGCTGACTCGGAAGCA (RP)	62
Atp1b1 (Na^+,K^+-ATPase β1)	NM_009721	TTCATCGGGACCATCCAAGT (FP) TCCTGGTATGTGGGCTTCAGT (RP)	62
Atp1b2 (Na^+,K^+-ATPase β2)	NM_013415	TGCCCACACAATTTCCAACAT (FP) ACTCCCGACTCCTCTCTGTCTCT (RP)	64
Atp1b3 (Na^+,K^+-ATPase β3)	NM_007502	GCCGAGTGGAAGCTGTTCAT (FP) GGTGCGCCCCAGAAACT (RP)	56
Atp1b4 (Na^+,K^+-ATPase β4)	NM_133690	TGAAAATGACATTCGATCCATCA (FP) TAAGGGTAGTAGCGGAGGTCAAA (RP)	69
Polr2a	NM_009089	GGCAAGGTCCCACAACCA (FP) ACAATTGATGTGTCCAGGTATGATG (RP)	93

FP: forward primer, RP: reverse primer, bp: base pair

Figure Legends

Figure 1. Gene targeting strategy. An *Atp1b1* gene targeting vector was made by floxing exon 4, introducing a PGK-Neo^R positive selection marker upstream of the 3′ loxP site, and placing an HSV-*tk* negative selection marker in a 3′-flanking position in the genomic fragment. The *Atp1b1* conditional knockout vector (ckv) was introduced into W2 embryonic stem cells and clones that had undergone homologous recombination were identified by Southern blot using a flanking probe (3′ FP) binding a 6.5 kb Xba I fragment from the targeted allele and a 10.2 kb fragment from the wildtype (wt) allele. Positive clones were then verified by PCR with primers amplifying a 3.0 kb portion on the 5′ side of the targeted allele. After karyotyping of positive ES cell clones, chimeric mice were produced. Germline-transmitting chimeras were bred to FLPeR mice to remove the FRT-flanked PGK-Neo^R selection marker, generating mice harboring the final floxed *Atp1b1* allele (*Atp1b1*$^{F/F}$). Cre/loxP-mediated deletion of exon 4 generates a deleted allele (*Atp1b1*$^{\Delta exon4}$) with an out-of-frame mutation that disrupts the coding sequence in exons 5 and 6.

Figure 2. Alveolar fluid clearance (AFC), lung permeability and wet-to-dry lung weight ratio (W/D) in β1 knockout mice. **A.** AFC (% per hour) in *Atp1b1*$^{Aqp5\text{-}cre}$ mice (13.6 ± 1.5) (n = 7) was significantly reduced compared to *Atp1b1*$^{F/F}$ mice (23.7 ± 2.6) (n = 7). **B.** AFC (% per hour) in *Atp1b1*$^{Sftpc\text{-}cre}$ mice (6.6 ± 1.5) (n = 4) was significantly reduced compared to *Atp1b1*$^{F/F}$ mice (29.8 ± 4.2) (n = 4). **C & D**. There was no significant difference in *in vivo* permeability to fluorescein-BSA between *Atp1b1*$^{F/F}$ (0.248 ± 0.047)

AJRCMB Articles in Press. Published on 11-April-2016 as 10.1165/rcmb.2016-0005OC

(n = 6) and *Atp1b1*$^{Aqp5\text{-}cre}$ mice (0.232 ± 0.055) (n = 7) (**C**) or between *Atp1b1*$^{F/F}$ (0.196 ± 0.020) (n = 6) and *Atp1b1*$^{Sftpc\text{-}cre}$ mice (0.227 ± 0.038) (n = 6) (**D**). **E & F**. At baseline, W/D of *Atp1b1*$^{F/F}$ (4.37 ± 0.15) (n = 8) versus *Atp1b1*$^{Aqp5\text{-}cre}$ (4.38 ± 0.05) (n = 12) mice (**E**) and of *Atp1b1*$^{F/F}$ (3.84 ± 0.08) (n = 6) versus *Atp1b1*$^{Sftpc\text{-}cre}$ (3.88 ± 0.08) (n = 6) mice (**F**) were not significantly different. ***P* < 0.01, NS = not significantly different from each other (*P* > 0.05).

Figure 3. Bioelectric properties and Na^+ absorption of β1 knockout MAECM. **A.** Transepithelial electrical resistance (R_T) across *Atp1b1*$^{F/F}$ MAECM (1.72 ± 0.09 kΩ·cm^2) (n = 42) was not significantly different compared to *Atp1b1*$^{Sftpc\text{-}cre}$ MAECM (1.95 ± 0.11 kΩ·cm^2) (n = 45) **B.** Equivalent short circuit current (I_{EQ}) was significantly lower in *Atp1b1*$^{Sftpc\text{-}cre}$ MAECM (3.81 ± 0.11 μA/cm^2) (n = 45) compared to *Atp1b1*$^{F/F}$ MAECM (7.00 ± 0.18) (n = 42). **C.** Unidirectional Na^+ fluxes in the apical-to-basolateral (A→B) direction were significantly lower in *Atp1b1*$^{Sftpc\text{-}cre}$ MAECM, while fluxes in the basolateral-to-apical (B→A) direction were unchanged (n = 3). **D.** Net Na^+ absorption of *Atp1b1*$^{F/F}$ and *Atp1b1*$^{Sftpc\text{-}cre}$ MAECM (n = 3) were significantly different with lower absorption in knockout monolayers. **P* < 0.05, ***P* < 0.01, ****P* < 0.001, NS = not significantly different from each other (*P* > 0.05).

Figure 4. Short-circuit current (I_{SC}) response to amiloride and pimozide. **A & B.** At t = 0, amiloride (10 μM) was added to apical fluid of *Atp1b1*$^{F/F}$ MAECM (n=3) (**A**) and *Atp1b1*$^{Sftpc\text{-}cre}$ MAECM (n=3) (**B**). After 60 minutes, pimozide (10 μM) was added to

apical fluid. **C & D.** At t = 0, pimozide (10 μM) was added to apical fluid of *Atp1b1*$^{F/F}$ MAECM (n=3) (**C**) and *Atp1b1*$^{Sftpc\text{-}cre}$ MAECM (n=3) (**D**). After 60 minutes, amiloride (10 μM) was added to apical fluid.

Figure 5. Wet-to-dry lung weight ratios (W/D) in mice exposed to hyperoxia or subjected to ventilator-induced lung injury (VILI). **A.** W/D were not significantly different between floxed and knockout mice after hyperoxic injury (65 hours in >95% oxygen). W/D in *Atp1b1*$^{F/F}$ and *Atp1b1*$^{Aqp5\text{-}cre}$ mice were 6.70 ± 0.22 vs 6.66 ± 0.09 (n = 3) and in *Atp1b1*$^{F/F}$ and *Atp1b1*$^{Sftpc\text{-}cre}$ mice were 6.47 ± 0.30 vs 5.96 ± 0.40 (n = 3). **B.** No significant difference in W/D between genotypes was observed after either non-injurious (peak inspiratory pressure (PIP) = 20 cmH_2O) or injurious (PIP = 40 cmH_2O) ventilation. W/D in *Atp1b1*$^{F/F}$ and *Atp1b1*$^{Sftpc\text{-}cre}$ were 4.70 ± 0.11 vs 4.72 ± 0.02 (n = 3) after non-injurious ventilation and 6.12 ± 0.17 vs 6.57 ± 0.26 (n = 5) after VILI. $^{**}P < 0.01$, $^{***}P < 0.001$, NS = not significant from each other ($P > 0.05$).

Figure 6. Expression of Na pump subunits in *Atp1b1*$^{Sftpc\text{-}cre}$ knockout mice. **A.** Representative Western blots reveal that Na pump α1 subunit was unchanged, β1 was undetectable and β3 was increased in AT2 cells from knockout mice. The upper band in β1 blot appears to be non-specific. **B.** Deletion of Na pump β1 subunit significantly increased β3 protein in AT2 cells isolated from *Atp1b1*$^{Sftpc\text{-}cre}$ (KO) compared to *Atp1b1*$^{F/F}$ (F/F) mice (n = 3). **C & D.** Antibody staining of MAECM (day 6) for Na pump β3 subunit in *Atp1b1*$^{F/F}$ cells (**C**) and *Atp1b1*$^{Sftpc\text{-}cre}$ cells (**D**) shows increased expression in MAECM generated from β1 knockout mice. **E – H.** Relative mRNA expression of α

AJRCMB Articles in Press. Published on 11-April-2016 as 10.1165/rcmb.2016-0005OC

and β subunit genes in whole lung from **(E)** *Atp1b1*$^{Aqp5\text{-}cre}$ and **(F)** *Atp1b1*$^{Sftpc\text{-}cre}$ mice (n = 4), and **(G)** isolated AT2 cells (n = 3) and **(H)** MAECM from *Atp1b1*$^{Sftpc\text{-}cre}$ mice (n = 3). Levels are relative to expression in *Atp1b1*$^{F/F}$ control lung, isolated AT2 cells or MAECM. **P* < 0.05, ****P* < 0.001, ***P* < 0.01, NS = not significant from each other (*P* > 0.05).

Figure 7. AFC in the absence or presence of terbutaline and Western analysis of β_2-adrenergic receptor (β_2AR) expression in Na pump β1 knockout mice. **A.** AFC measurements in the absence of terbutaline demonstrated lower AFC in *Atp1b1*$^{Aqp5\text{-}cre}$ vs control mice. In contrast, terbutaline-stimulated AFC in *Atp1b1*$^{Aqp5\text{-}cre}$ mice reached 22.5 ± 2.6% per hour (n = 4), which was not significantly different from *Atp1b1*$^{F/F}$ control mice (27.3 ± 4.7% per hour, n = 4). **B.** AFC in the absence of terbutaline was significantly lower in *Atp1b1*$^{Sftpc\text{-}cre}$ vs control mice, while terbutaline-stimulated AFC in *Atp1b1*$^{Sftpc\text{-}cre}$ mice was 30.9 ± 1.0% per hour (n = 4), which was not significantly different from *Atp1b1*$^{F/F}$ control mice (36.4 ± 2.9% per hour, n = 4). **C & D.** Western analysis of β_2AR protein in whole lung in *Atp1b1*$^{Aqp5\text{-}cre}$ **(C)** and *Atp1b1*$^{Sftpc\text{-}cre}$ **(D)** mice shows increased expression in both knockout lines compared to *Atp1b1*$^{F/F}$ control mice. **P* < 0.05, ***P* < 0.01, NS = not significant from each other (*P* > 0.05).

Figure 1

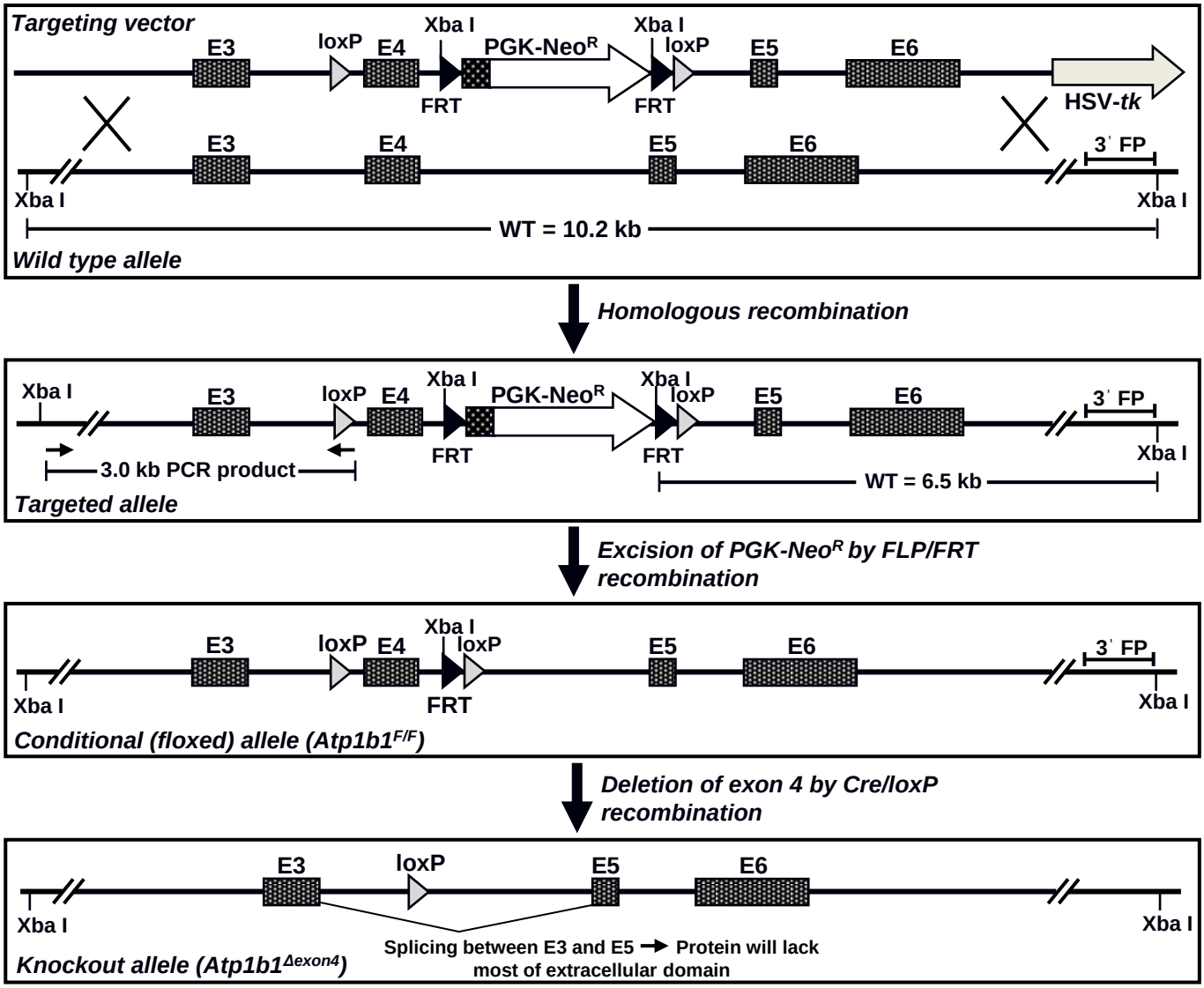

AJRCMB Articles in Press. Published on 11-April-2016 as 10.1165/rcmb.2016-0005OC

Figure 2

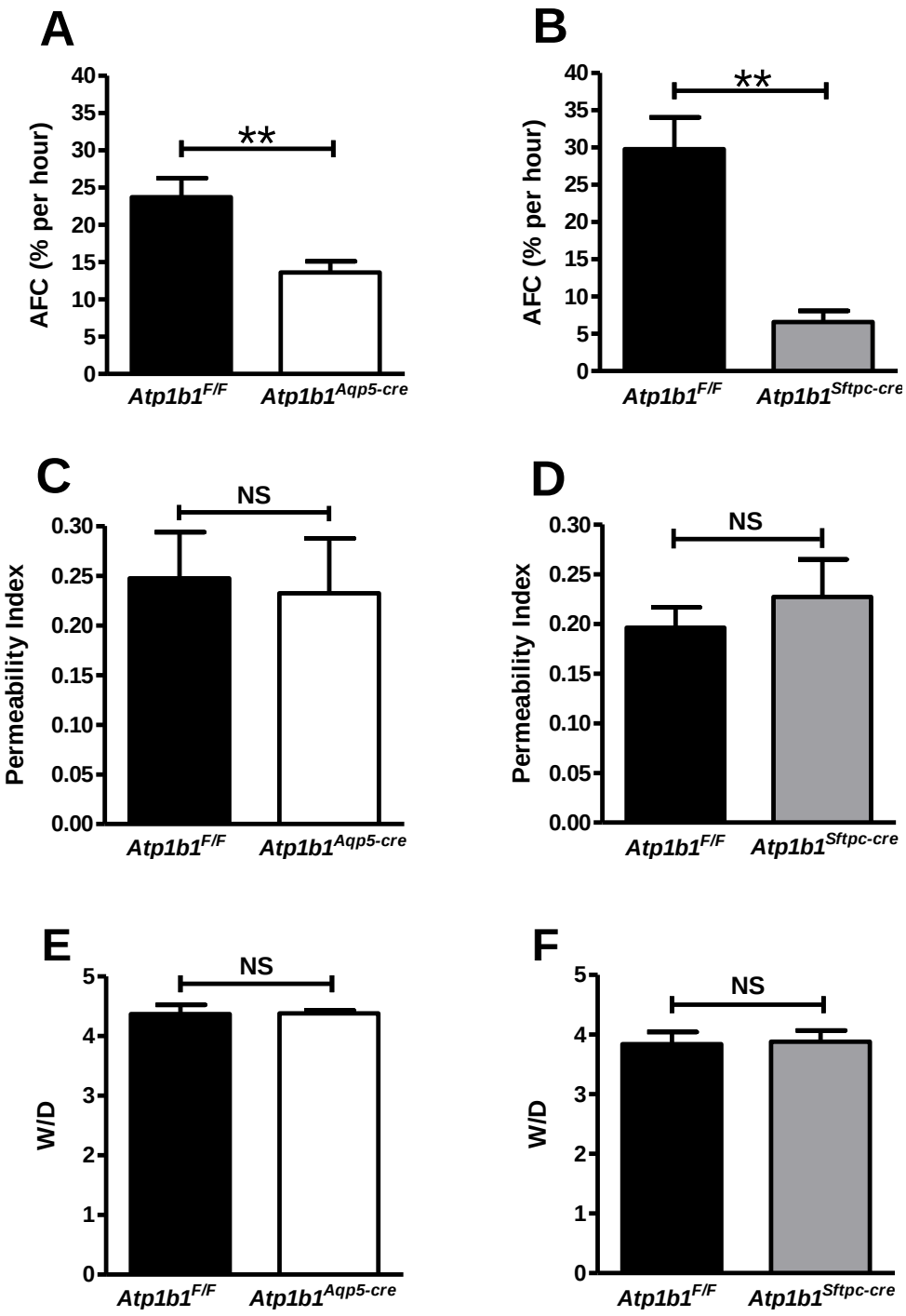

Figure 3

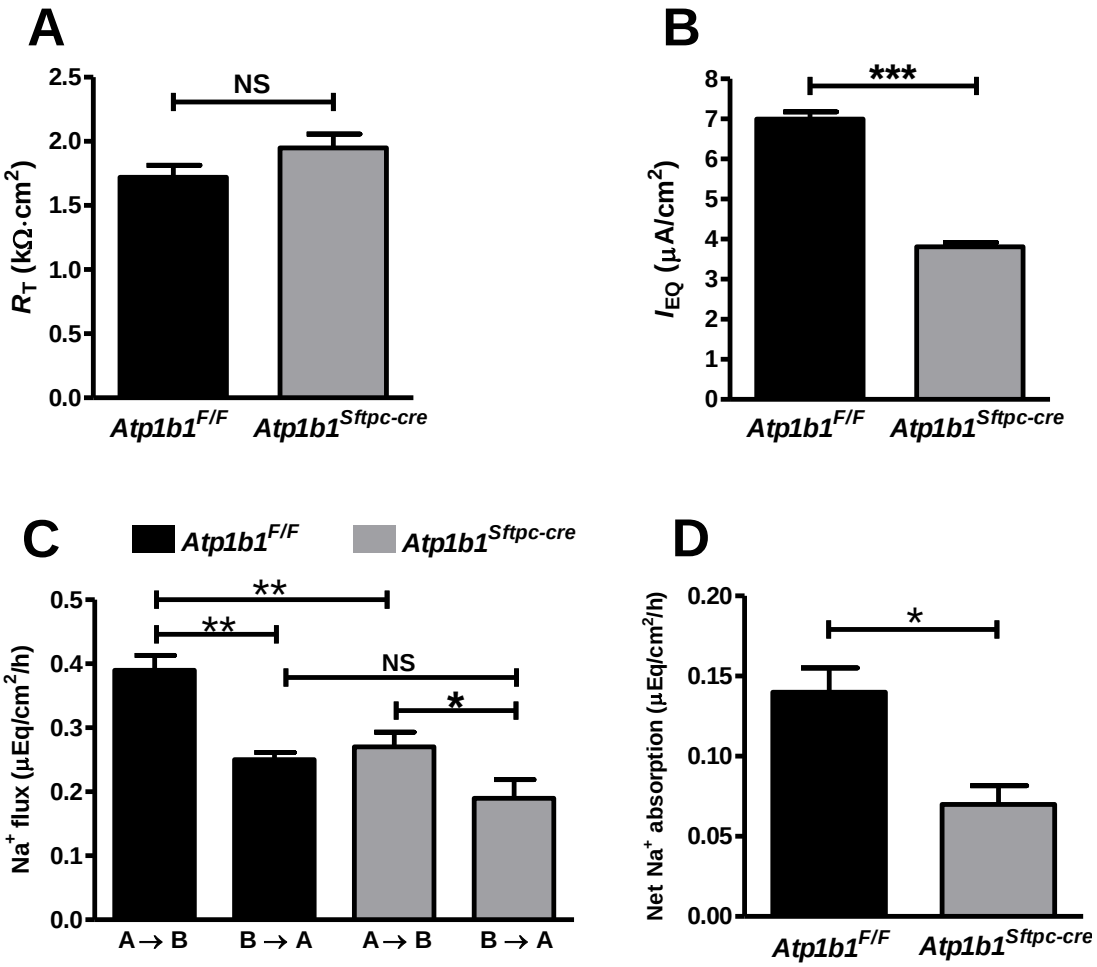

AJRCMB Articles in Press. Published on 11-April-2016 as 10.1165/rcmb.2016-0005OC

Figure 4

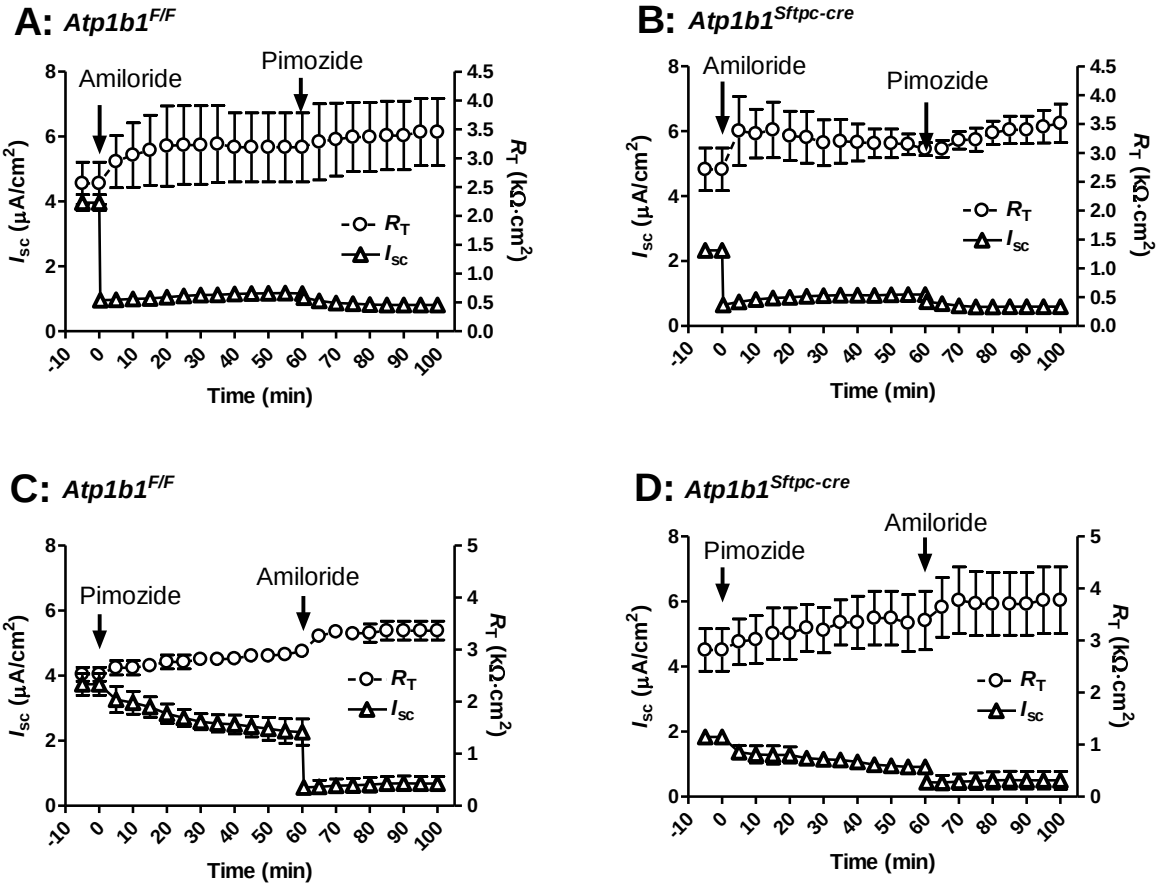

Figure 5

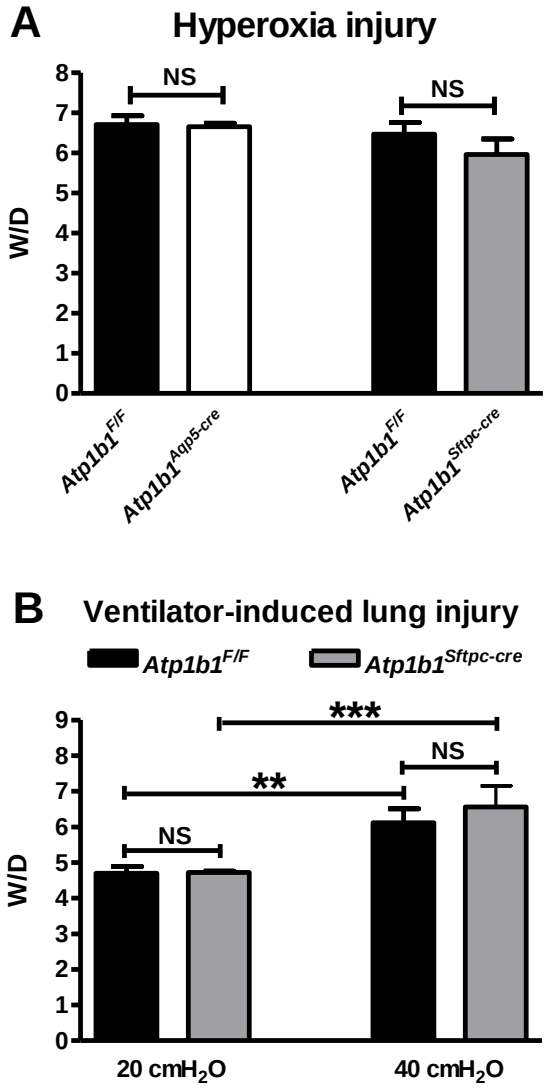

AJRCMB Articles in Press. Published on 11-April-2016 as 10.1165/rcmb.2016-0005OC

Figure 6

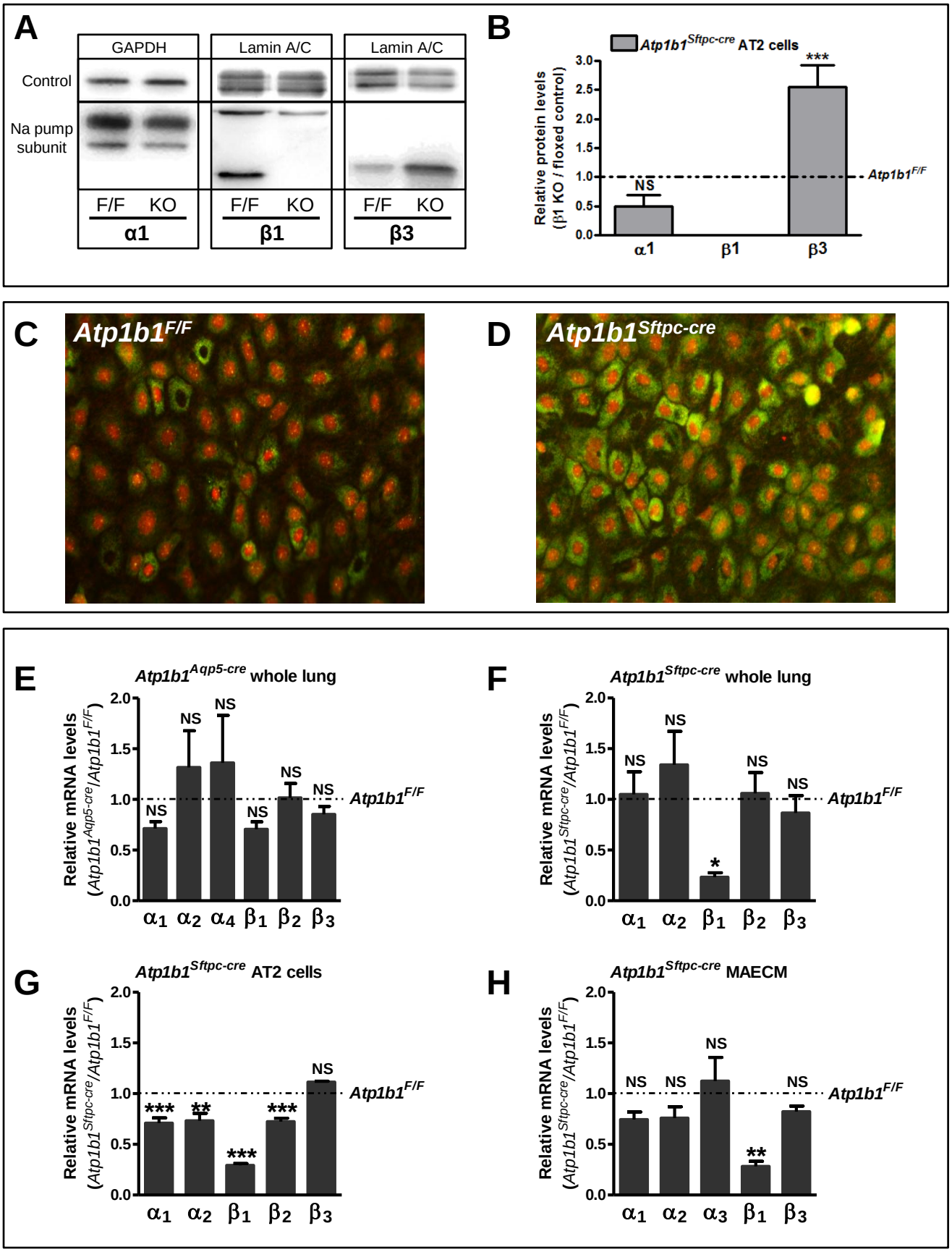

Figure 7

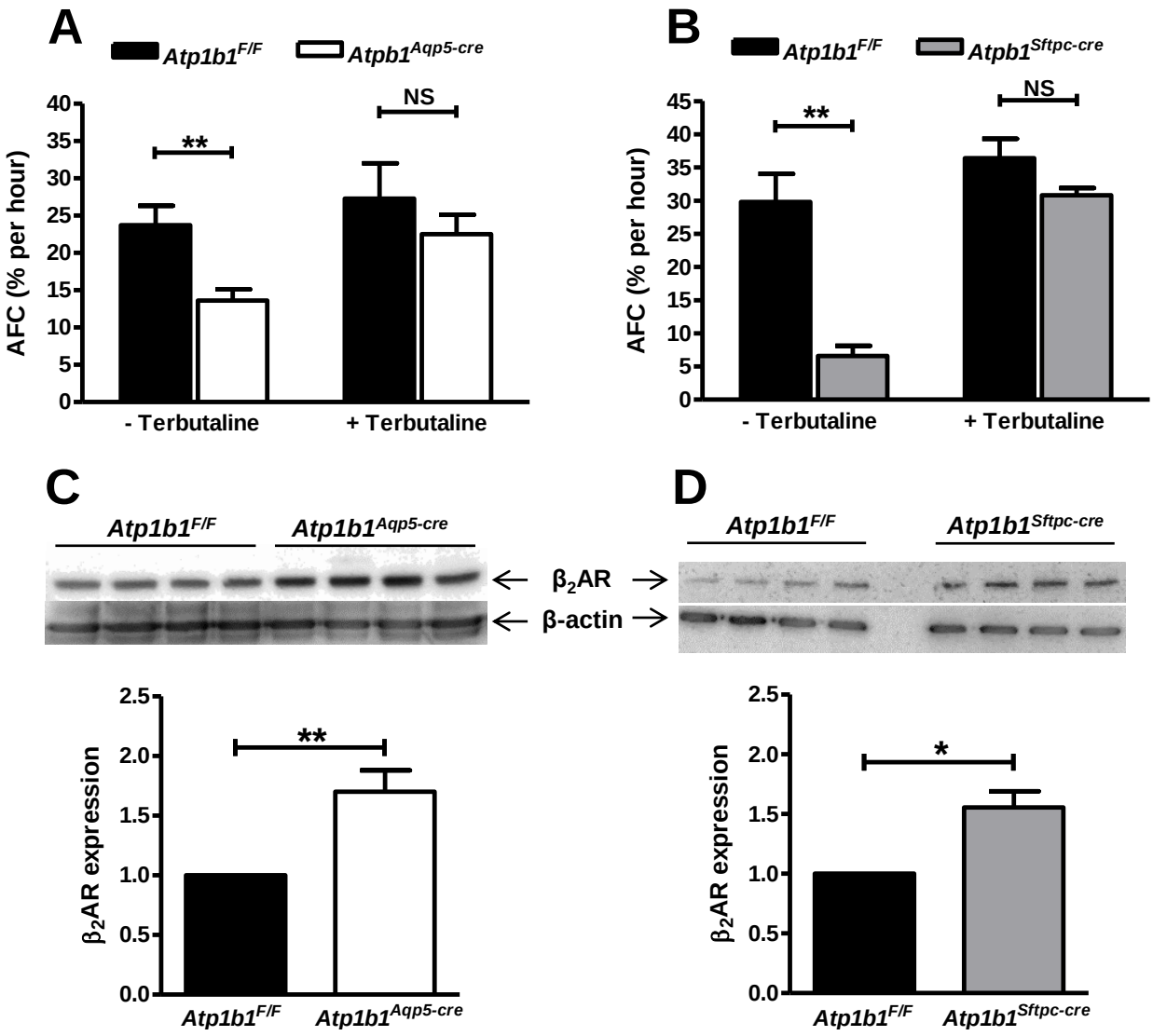

AJRCMB Articles in Press. Published on 11-April-2016 as 10.1165/rcmb.2016-0005OC

Online Supplement

Materials and Methods

Generation of knockout mice

Mice with a floxed allele of the Na pump β1 subunit gene (*Atp1b1*) were generated. For this purpose, a conditional (floxed) *Atp1b1* gene targeting vector was constructed by bacterial recombineering using methods and reagents provided by the National Cancer Institute, Fredrick, MD (http://ncifrederick.cancer.gov/research/brb/recombineeringInformation.aspx) (1, 2). A Bacterial Artificial Chromosome (BAC) clone containing the *Atp1b1* gene was obtained after screening a mouse BAC library (RPCI-22, derived from mouse strain 129S6/SvEvTac) from Children's Hospital Oakland Research Institute, Oakland, CA. An 8,387 bp genomic *Atp1b1* fragment, representing the sequence starting 1,471 bp upstream of exon 3, was retrieved from the BAC clone into PL253, a pBluescript II SK vector containing Herpes Simplex Thymidine Kinase (HSV-*tk*) for negative selection. LoxP sites were subsequently inserted by bacterial homologous recombination to flank exon 4 of the *Atp1b1* gene, together with an FRT-flanked phosphoglycerate kinase promoter-Neomycin resistance (PGK-Neo^R) marker for positive selection. The construct was introduced into W4 ES cells (derived from mouse strain 129S6/SvEvTac), and positive clones that had gone through homologous recombination were identified by Southern blot hybridization with a flanking probe and verified by PCR. Positive clones with correct karyotype were injected into C57BL/6J host blastocysts and chimeric males were generated. Germline-transmitting chimeras were bred to FLPeR mice (3), strain 129S4/SvJaeSor-*Gt(ROSA)26Sor*$^{tm1(FLP1)Dym}$/J, stock #003946, Jackson Laboratories, Bar Harbor, MA, to remove the FRT-flanked PGK-Neo^R selection marker. Resultant

floxed *Atp1b1* mice (*Atp1b1*$^{F/F}$) were backcrossed to 129S6/SvEvTac mice for 10 generations and then crossed to *Aqp5-cre* mice (also on 129S6/SvEvTac background), a line recently established in our laboratory (4), to generate mice deficient in the β1 subunit in AT1 cells (called *Atp1b1*$^{Aqp5\text{-}cre}$). In order to knock out the β1 subunit in the entire alveolar epithelium (i.e., both AT1 and AT2 cells), *Atp1b1*$^{F/F}$ mice were crossed to *Sftpc-cre* mice (on C57BL/6 genetic background) to generate *Atp1b1*$^{Sftpc\text{-}cre}$ mice. The *Sftpc-cre line* has been described previously (5) and was generously provided by Brigid Hogan, Duke University, Durham, NC. Therefore, *Atp1b1*$^{Aqp5\text{-}cre}$ and the corresponding *Atp1b1*$^{F/F}$ control mice were on a pure 129S6/SvEvTac background, while *Atp1b1*$^{Sftpc\text{-}cre}$ and *Atp1b1*$^{F/F}$ controls were on a mixed 129S6/SvEvTac:C57BL/6J background. Specificity and efficiency of the Cre transgenes in both lines was verified by crosses to the Cre-dependent reporter line *ROSA*$^{mT/mG}$ (6), purchased from Jackson Laboratories (strain Gt(ROSA)26Sor$^{tm4(ACTB\text{-}tdTomato,\text{-}EGFP)Luo}$/J). For GFP reporter expression analysis, lungs were fixed/frozen and cryosectioned as described (6) and analyzed by confocal microscopy. Initially, we used *Nkx2.1-cre* mice (7) to generate an alveolar epithelium-specific β1 knockout line. The *Nkx2.1-cre* line was kindly provided by Stewart A. Anderson (Cornell University, New York, NY). Since *Atp1b1*$^{Nkx2.1\text{-}cre}$ mice died postnatally at 2-3 weeks of age, *Atp1b1*$^{Sftpc\text{-}cre}$ mice were used in this study. All animal protocols were approved by the Institutional Animal Care and Use Committee (IACUC) at the University of Southern California.

Verification of Atp1b1 gene deletion

AJRCMB Articles in Press. Published on 11-April-2016 as 10.1165/rcmb.2016-0005OC

Verification of correct Cre/loxP-mediated deletion of exon 4 in the floxed *Atp1b1* allele (*Atp1b1*$^{F/F}$) was performed by PCR amplification. Genomic DNA isolated from lungs of *Atp1b1*$^{Aqp5\text{-}cre}$ mice was used as template to amplify a predicted 343 bp PCR product from the deleted allele (*Atp1b1*$^{\Delta exon4}$), along with a 1226 bp product amplified from the intact *Atp1b1*$^{F/F}$ allele. The following PCR primers flanking exon 4 were used: forward (P1): 5'-GGGTCACCACAACATGAGGAACTA-3', reverse (P2): 5'-TGGTTATCAAAGGGCAGAGACCGT-3').

Alveolar fluid clearance (AFC)

AFC was measured according to previously published methods (8, 9). Mice 3-5 months old and 20-30 grams were used. Animals were sedated with diazepam, anesthetized with pentobarbital and placed supine on a warming pad. An incision was made in the neck area, trachea was exposed and transected, and a 20-gauge plastic catheter (Angiocath #381702, BD Infusion Therapy Systems, Sandy, UT) was inserted into the trachea for administration of an instillate comprised of 5% bovine serum albumin (BSA, Sigma-Aldrich, St Louis, MO) plus 0.025% Alexa Fluor 594-conjugated BSA (Life Technologies, Carlsbad, CA) in phosphate-buffered saline (PBS). Before instillation, mice were paralyzed with pancuronium bromide (1 mg/kg) and mechanically ventilated with an Inspira ASV ventilator (Harvard Apparatus, Holliston, MA) with 100% O_2 at tidal volume (V_t) = 10 ml/kg, 150 breaths per minute (bpm), peak inspiratory pressure (PIP) = 12 cmH_2O and positive-end expiratory pressure (PEEP) = 3 cmH_2O. Arterial O_2 saturation and heart rate were measured continuously using a MouseOx (Starr Life Sciences, Oakmont, PA). Using the tracheal catheter, 12 ml instillate/kg of body weight

was administered and, after 30 minutes, fluid was aspirated. Fluorescence (excitation at 590 nm) in the instillate (F_i) and aspirate (F_a) was measured at an emission wavelength of 622 nm and used for AFC (%/hour) calculation as $(1 - F_i/F_a) \times 100 \times 2$.

In vivo lung permeability

Measurement of alveolar epithelial permeability *in vivo* was performed as described previously (10) using fluorescein-labeled BSA (F-BSA, Life Technologies). Animals were anesthetized with Ketamine/Xylazine (100 mg/kg and 20 mg/kg, respectively) and 10 mg/kg body weight of F-BSA (1 mg/ml) was injected into the jugular vein. Mice were then kept anesthetized during the following 2 hour period by re-administration of Ketamine (50 mg/kg). Two hours after injection of F-BSA, bronchoalveolar lavage fluid (BALF) and blood was collected. Blood was obtained by heart puncture and after coagulation for 30 min at room temperature and subsequent centrifugation at 1,300 x *g* for 10 minutes, serum was collected. BALF was obtained by lavaging lungs three times with PBS (30 µl per kg body weight). The three BALF samples were pooled and centrifuged for 10 minutes at 600 x *g* at 4°C to pellet cells and the supernatant was collected. Fluorescence in BALF supernatant and serum (diluted 100-fold in PBS) was measured using excitation/emission wavelengths of 494/520 nm. Lung permeability index was defined as the ratio between the fluorescence observed in undiluted BALF supernatant and that in 1:100 diluted serum.

Wet-to-dry lung weight ratios

AJRCMB Articles in Press. Published on 11-April-2016 as 10.1165/rcmb.2016-0005OC

Lungs were surgically removed, weighed and then dried at 65°C for 48 hours. Dry weight was recorded and wet-to-dry lung weight ratios were calculated.

Isolation of AT2 cells and primary culture of mouse alveolar epithelial cell monolayers (MAECM)

AT2 cells were isolated from Na-K-ATPase β1 subunit knockout (*Atp1b1*$^{Sftpc\text{-}cre}$) and floxed control (*Atp1b1*$^{F/F}$) mice (20-30 grams) according to our previously established laboratory protocols (11). Briefly, after mice were anesthetized with a lethal dose of Euthasol, lungs were cleared of blood by cardiac perfusion with PBS. Dispase (BD Biosciences, Bedford, MA) was instilled into lungs via the trachea, followed by 0.5 ml of 1% low-melting-point agarose (Sigma, St. Louis, MO). Lungs were excised and incubated in dispase for 45 minutes at room temperature. Lungs were dissected into wash medium (1:1 mixture of Dulbecco's modified Eagle's medium and Ham's F-12 (DMEM/F-12; Sigma) supplemented with 0.01% DNase, 10 mM HEPES (Sigma-Aldrich), 0.1 mM nonessential amino acids (Sigma-Aldrich), 1 mM L-glutamine (Sigma-Aldrich) and 0.2% Primocin (InvivoGen, San Diego, CA)). Lung pieces were chopped and the resulting crude cell mixture was passed through a series of Nitex filters (100, 40, 20 and 10 μm; Tetko, Elmsford, NY), followed by centrifugation at 300 x *g* for 10 minutes at 4°C. Erythrocytes and macrophages were removed from this crude cell mixture by incubation with biotinylated antibodies (anti-CD45, anti-Ter 119, and anti-CD16/32; BD Biosciences), followed by selection with streptavidin-conjugated magnetic beads (Promega, Madison, WI). Partially purified cell mixtures were then incubated on Petri dishes precoated with mouse IgG (Sigma-Aldrich) for 2 hours at 37°C.

Nonadherent AEC were removed from IgG plates. Purified AT2 cells were resuspended in complete mouse medium (CMM): DMEM/F-12 supplemented with 1 mM L-glutamine, 0.25% BSA (BD Biosciences), 10 mM HEPES, 0.1 mM nonessential amino acids, 0.05% insulin-transferrin-sodium selenite (ITS; Roche, Basel, Switzerland) and 0.2% Primocin. Purified AT2 cells in CMM supplemented with 2% newborn bovine serum (Omega Scientific, Tarzana, CA) were plated onto tissue culture-treated polycarbonate filters (0.4 μm pores, 1.13 cm^2; Corning Costar, Cambridge, MA) precoated with laminin-5 (1 μg/ml; Millipore, Billerica, MA) at $7.5x10^5$ cells/cm^2. Cells were maintained at 37°C in a humidified atmosphere of 5% CO_2 + 95% air. Confluent monolayers formed by day 3 in primary culture. MAECM exhibit alveolar epithelial type I cell-like morphology and phenotype (11). Cells were fed with serum-free CMM every other day starting on day 3.

Bioelectric properties of MAECM

Transepithelial electrical resistance (R_T; $k\Omega \cdot cm^2$) and spontaneous potential difference (*PD*; mV) were measured using a Millicell-ERS (Millipore) device. Background R_T and *PD* were measured using blank filters and used to correct for measured R_T and *PD*. Equivalent short-circuit current (I_{EQ}; μA/cm^2) was calculated as PD/R_T using background-corrected values. R_T and *PD* were measured until day 10 after plating, starting from day 3 in culture. For measurements of short-circuit current (I_{SC}; μA/cm^2) in response to amiloride (10 μM; Sigma-Aldrich) or pimozide (10 μM; Sigma-Aldrich), monolayers were mounted in modified Ussing chambers and bathed on both sides with ITS-free CMM at 37°C. A stream of humidified 5% CO_2 in air was continuously blown

AJRCMB Articles in Press. Published on 11-April-2016 as 10.1165/rcmb.2016-0005OC

across surfaces of the bathing fluids (10 ml) to maintain constant pH and agitate bathing fluids. Monolayers were continuously short-circuited throughout the experimental period, except for brief interruptions (at 5 minute intervals) to allow measurements of *PD*. R_T of short-circuited monolayers was estimated intermittently as PD/I_{SC}.

Unidirectional flux of Na^+

Unidirectional flux of Na^+ was determined in the apical-to-basolateral (A→B) and basolateral-to-apical (B→A) directions across MAECM at 37°C using ^{22}NaCl (American Radiolabeled Chemicals, St. Louis, MO). Briefly, ^{22}NaCl (with a final specific activity of 0.5 μCi/ml) was added to the upstream (either apical or basolateral) fluid of monolayers mounted in modified Ussing chambers. During measurements of unidirectional Na^+ fluxes, monolayers were short-circuited to eliminate electrical gradients across the alveolar epithelial barrier. Downstream samples were taken at 30 minute intervals for up to 120 minutes. Aliquots of upstream fluid were taken at 10 minutes after ^{22}NaCl addition and at the end of each experiment. Samples were mixed with 10 ml of Ecoscint (National Diagnostics, Manville, NJ) and assayed for radioactivity in a liquid scintillation counter (LS 6000TA, Beckman, Fullerton, CA).

Western analysis

Whole lung lysates for Western analysis were prepared as follows: lungs were cleared of blood by transcardiac perfusion with PBS and homogenized on ice with a Polytron homogenizer in lysis buffer (2% SDS/10% glycerol/62.5 mM Tris, pH 6.8) including protease inhibitors (Protease Inhibitor Cocktail Set III, Millipore). After further lysis for 1

hour on ice and 15 minutes at 37°C, DNA was sheared by passing samples 5 times through a 25-gauge needle. Debris was removed by centrifugation for 15 minutes at 20,000 x *g* at 4°C. Lysates (supernatants) were stored at -80°C in aliquots. Protein from freshly isolated AT2 cells was prepared as above with the exception that the Polytron homogenizer was replaced by vortexing. Protein concentrations in all samples were measured with the Bio-Rad DC Protein Assay Kit (Bio-Rad, Hercules, CA). Protein samples to be subjected to Western analysis of Na-K-ATPase β subunit expression were deglycosylated with PNGase F (New England Biolabs, Ipswich, MA) according to the manufacturer's protocol. For Western analysis, equal amounts of protein in sample buffer (20-60 μg) were resolved by 10% SDS-PAGE under reducing conditions using the buffer system of Laemmli (12) and transferred to Immobilon-P membranes (Millipore). Membranes were blocked in 5% nonfat dry milk in Tris-buffered saline with 0.1% Tween 20 for 60 minutes and incubated overnight at 4°C with primary antibody. The following primary antibodies were used: rabbit anti-α1 subunit of Na-K-ATPase (#06-520, Millipore), rabbit anti-β1 subunit of Na-K-ATPase (#GTX113390, GeneTex Irvine, CA), goat anti-β3 subunit of Na-K-ATPase (sc-66343, Santa Cruz Biotechnology, Dallas, TX) and rabbit anti-β_2 adrenergic receptor (#ab36956, Abcam, Cambridge, MA). The following antibodies were used for sample normalization purposes: rabbit anti-lamin A/C (#sc20681, Santa Cruz Biotechnology), mouse anti-glyceraldehyde 3-phosphate dehydrogenase (GAPDH, #AM4300, Life Technologies) and mouse anti-actin (#ab6276, Abcam). After washing, membranes were incubated with species-specific secondary antibodies (anti-rabbit, -goat or -mouse IgG) conjugated to horseradish peroxidase for 1 hour at room temperature, and antigen-antibody complexes were visualized by

AJRCMB Articles in Press. Published on 11-April-2016 as 10.1165/rcmb.2016-0005OC

enhanced chemiluminescence (Pierce, Rockford, IL) using the FluorChem Imaging System (Model 8900, Alpha Innotech, San Leandro, CA), which was also used for quantitation of specific protein bands and loading controls for normalization.

Lung histology

Lungs were cleared of blood by cardiac perfusion with PBS and then inflated with 4% paraformaldehyde (PFA) in PBS at 20 cmH_2O pressure. When pressure was stable, the trachea was tied off with surgical sutures. Lungs were then immersed in 4% PFA in PBS and fixed at 4°C for 16-20 hours. After embedding in paraffin, 5 μm sections were cut and stained with hematoxylin and eosin (H&E).

Antibody staining

Na pump β3 subunit protein in MAECM was identified by immunofluorescence microscopy using a rabbit polyclonal β3 antibody (generously provided by Alicia McDonough, USC, CA). Briefly, MAECM on day 6 were rinsed with ice-cold PBS, fixed with 4% paraformaldehyde for 15 minutes and rinsed in PBS. Antigen retrieval was performed in Antigen Unmasking Solution, High pH (#H-3301, Vector Laboratories, Burlingame, CA). After permeabilization with 0.2% Triton X-100 in Tris-buffered saline with 0.1% Tween 20 (TBS-T) for 15 minutes at room temperature and rinses in TBS-T, MAECM were incubated in CAS Block (Life Technologies) plus 5% donkey serum for 1 hour at room temperature. Next, MAECM were incubated with the β3 antibody (diluted 1:1,000 in CAS Block) on a rocker overnight at 4°C. After washes in TBS-T, MAECM were incubated with secondary antibody (Alexa Fluor 488-conjugated donkey anti-rabbit

IgG (H+L), Life Technologies, diluted 1:500 in CAS Block) for 1 hour at room temperature on a rocker. After washes in TBS-T, MAECM were placed on glass slides, one drop of propidium iodide (PI) mounting media was added and coverslips placed on top. Stained specimens were viewed with an epifluorescence microscope (BX60, Olympus, Tokyo, Japan).

RNA isolation, reverse transcription (RT) and quantitative polymerase chain reaction (qPCR)

Total RNA was extracted from whole lungs, freshly isolated AT2 cells or MAECM using TRIzol (Life Technologies). RNA was quantified spectrophotometrically by determining absorption at 260 nm (A_{260}) and calculating concentration (µg/ml) from A_{260} x 40 x sample dilution factor. RNA purity was calculated from A_{260}/A_{280}. Integrity of RNA was checked by agarose gel electrophoresis prior to RT. RNA was reverse transcribed into complementary DNA (cDNA) using ThermoScript RT-PCR System (Life Technologies) with random hexamer primers as follows: incubation of 2 µg RNA at 65°C for 5 minutes, at 50°C for 50 minutes and at 85°C for 5 minutes. In parallel, RT reactions without reverse transcriptase were performed as control for contaminating genomic DNA. cDNA was analyzed by SYBR-Green qPCR using a 7900HT Fast Real-Time PCR System (Applied Biosystems, Carlsbad, CA). Primers were designed using Primer Express 3.0 software (Applied Biosystems) and tested for specificity by dissociation analysis. PCR mixtures consisted of 0.5 µl cDNA, 10 µl SYBRGreen (Applied Biosystems), 5.5 µl PCR-water and 4 µl primer mix (2 µM forward and reverse primer). The qPCR procedure was comprised of three components; pre-amplification denaturation (one cycle at 50°C for 2

AJRCMB Articles in Press. Published on 11-April-2016 as 10.1165/rcmb.2016-0005OC

minutes and at 95°C for 10 minutes), amplification (40 cycles at 95°C for 15 seconds and at 60°C for 1 minute) and post-amplification (one cycle at 95°C for 15 seconds, at 60°C for 15 seconds, and at 95°C for 15 seconds). Sequences of all primers used, along with the expected product size and accession numbers, are shown in Table 1. *Polr2a* (RNA polymerase II α subunit), a housekeeping gene, was used as internal control.

Hyperoxia exposure

Mice were housed in cages with free access to food and water inside a hyperoxia chamber (Terra Universal, Fullerton, CA) for 65 hours. Sodium bicarbonate (Sigma-Aldrich) was used to absorb exhaled carbon dioxide. Oxygen concentration inside the chamber was continuously monitored with a MiniOX I Oxygen Analyzer (Ohio Medical, Gurnee, IL) and maintained at >95% at a flow of 15 l/hour (Visi-Float Flowmeter VFA, Dwyer Instruments, Michigan City, IN).

Ventilator-induced lung injury (VILI)

VILI was performed as previously described (13, 14). Mice of the same age and weight ranges as those used for AFC experiments (see above) were anesthetized with Ketamine/Xylazine (100/20 mg/kg, i.p.). An incision was made in the neck area, trachea was exposed and transected, and a 20-gauge plastic catheter (BD Infusion Therapy Systems) was inserted. The catheter was secured inside the trachea with surgical suture, after which the incision was closed. Mice were then placed in supine position on a warming pad (37°C) on a flat platform and connected to an Inspira ASV ventilator

(Harvard Apparatus). Non-injurious ventilation (room air) was performed for 3 hours with PIP = 20 cmH_2O, PEEP = 0 cmH_2O and respiratory rate = 70 bpm. Injurious ventilation (VILI) was performed for 3 hours with PIP = 40 cmH_2O, PEEP = 0 cmH_2O and respiratory rate = 25 bpm. Animals were monitored throughout the experiment by measuring arterial O_2 saturation and heart rate with a MouseOx device (Starr Life Sciences). As needed, mice were re-anesthetized with 50 mg Ketamine/kg body weight, based on increases in heart rate (approximately every 30 minutes).

Data analysis

Data are shown as mean ± SEM (standard error of the mean). Unpaired, two-tailed Student's *t*-test was used for comparisons of two group means. Multiple (≥3) group means were analyzed by one-way analysis of variance (ANOVA) with post-hoc tests based on Student-Newman-Keuls approaches. P <0.05 is considered statistically significant.

Results

Figure Legends

Figure E1. Verification of Na pump β1 subunit deletion. **A.** Verification of knockout in $Atp1b1^{Aqp5\text{-}cre}$ lung. Deletion of exon 4 in the floxed allele ($Atp1b1^{F/F}$) by Cre generates the deleted allele $Atp1b1^{\Delta exon4}$. PCR amplification of genomic DNA from $Atp1b1^{F/F}$ lung with primers P1 and P2 results in a 1226 bp product (lane "1"), while the deleted allele present in $Atp1b1^{Aqp5\text{-}cre}$ lung is amplified as a 343-bp product (lane "2") using the same primers. The $Atp1b1^{F/F}$ (1226 bp) product in lane 2 is contributed by cells not expressing

AJRCMB Articles in Press. Published on 11-April-2016 as 10.1165/rcmb.2016-0005OC

Cre in the lung. M = 100 bp ladder. **B**. Verification of knockout by Western analysis of Na pump β1 subunit protein in AT2 cells isolated from *Atp1b1*$^{Sftpc\text{-}cre}$ (KO) and *Atp1b1*$^{F/F}$ (F/F) mice. Results from three separate cell isolations (#1-3) are shown. In each cell isolation experiment, AT2 cells from two mice of each genotype were pooled. **C.** Activity of Cre lines used to generate knockouts of *Atp1b1*. Left panel: In *Aqp5*^{cre};*ROSA*$^{mT/mG}$ double transgenic mice, *Aqp5*^{cre} activates GFP (*mG*) expression from the *ROSA*$^{mT/mG}$ reporter transgene specifically in AT1 cells in the alveolar epithelium. Red fluorescence represents Tomato (*mT*) reporter in cells not expressing Cre (i.e., AT2, endothelial and other cells). Right panel: In *Sftpc*^{cre};*ROSA*$^{mT/mG}$ double transgenic mice, *Sftpc*^{cre} activates GFP expression from the *ROSA*$^{mT/mG}$ reporter transgene in both AT1 and AT2 cells, although the GFP signal is considerably stronger in AT2 cells. Tomato reporter is observed in cells not expressing Cre (i.e., endothelial and other cells). Blue is DAPI (nuclear).

Figure E2. Lung histology. No apparent differences were observed in distal lung histology between *Atp1b1*$^{F/F}$ and *Atp1b1*$^{Aqp5\text{-}cre}$ lungs (upper panels) or between *Atp1b1*$^{F/F}$ and *Atp1b1*$^{Sftpc\text{-}cre}$ lungs (lower panels).

References

1. Copeland NG, Jenkins NA, Court DL. Recombineering: a powerful new tool for mouse functional genomics. *Nat Rev Genet* 2001; 2: 769-779.

2. Liu P, Jenkins NA, Copeland NG. A highly efficient recombineering-based method for generating conditional knockout mutations. *Genome Res* 2003; 13: 476-484.

3. Farley FW, Soriano P, Steffen LS, Dymecki SM. Widespread recombinase expression using FLPeR (flipper) mice. *Genesis* 2000; 28: 106-110.

4. Flodby P, Borok Z, Banfalvi A, Zhou B, Gao D, Minoo P, Ann DK, Morrisey EE, Crandall ED. Directed expression of Cre in alveolar epithelial type 1 cells. *Am J Respir Cell Mol Biol* 2010; 43: 173-178.

5. Okubo T, Knoepfler PS, Eisenman RN, Hogan BL. Nmyc plays an essential role during lung development as a dosage-sensitive regulator of progenitor cell proliferation and differentiation. *Development* 2005; 132: 1363-1374.

6. Muzumdar MD, Tasic B, Miyamichi K, Li L, Luo L. A global double-fluorescent Cre reporter mouse. *Genesis* 2007; 45: 593-605.

7. Xu Q, Tam M, Anderson SA. Fate mapping Nkx2.1-lineage cells in the mouse telencephalon. *J Comp Neurol* 2008; 506: 16-29.

8. Mutlu GM, Dumasius V, Burhop J, McShane PJ, Meng FJ, Welch L, Dumasius A, Mohebahmadi N, Thakuria G, Hardiman K, Matalon S, Hollenberg S, Factor P. Upregulation of alveolar epithelial active Na^+ transport is dependent on β2-adrenergic receptor signaling. *Circ Res* 2004; 94: 1091-1100.

AJRCMB Articles in Press. Published on 11-April-2016 as 10.1165/rcmb.2016-0005OC

9. Hardiman KM, Lindsey JR, Matalon S. Lack of amiloride-sensitive transport across alveolar and respiratory epithelium of iNOS$^{-/-}$ mice in vivo. *Am J Physiol Lung Cell Mol Physiol* 2001; 281: L722-L731.

10. Han X, Fink MP, Uchiyama T, Yang R, Delude RL. Increased iNOS activity is essential for pulmonary epithelial tight junction dysfunction in endotoxemic mice. *Am J Physiol Lung Cell Mol Physiol* 2004; 286: L259-L267.

11. DeMaio L, Tseng W, Balverde Z, Alvarez JR, Kim KJ, Kelley DG, Senior RM, Crandall ED, Borok Z. Characterization of mouse alveolar epithelial cell monolayers. *Am J Physiol Lung Cell Mol Physiol* 2009; 296: L1051-L1058.

12. Laemmli UK. Cleavage of structural proteins during the assembly of the head of bacteriophage T4. *Nature* 1970; 227: 680-685.

13. Kage H, Flodby P, Gao D, Kim YH, Marconett CN, DeMaio L, Kim KJ, Crandall ED, Borok Z. Claudin 4 knockout mice: normal physiological phenotype with increased susceptibility to lung injury. *Am J Physiol Lung Cell Mol Physiol* 2014; 307: L524-536.

14. Li G, Flodby P, Luo J, Kage H, Sipos A, Gao D, Ji Y, Beard LL, Marconett CN, DeMaio L, Kim YH, Kim KJ, Laird-Offringa IA, Minoo P, Liebler JM, Zhou B, Crandall ED, Borok Z. Knockout mice reveal key roles for claudin 18 in alveolar barrier properties and fluid homeostasis. *Am J Respir Cell Mol Biol* 2014; 51: 210-222.

AJRCMB Articles in Press. Published on 11-April-2016 as 10.1165/rcmb.2016-0005OC

Figure E1 (online supplement)

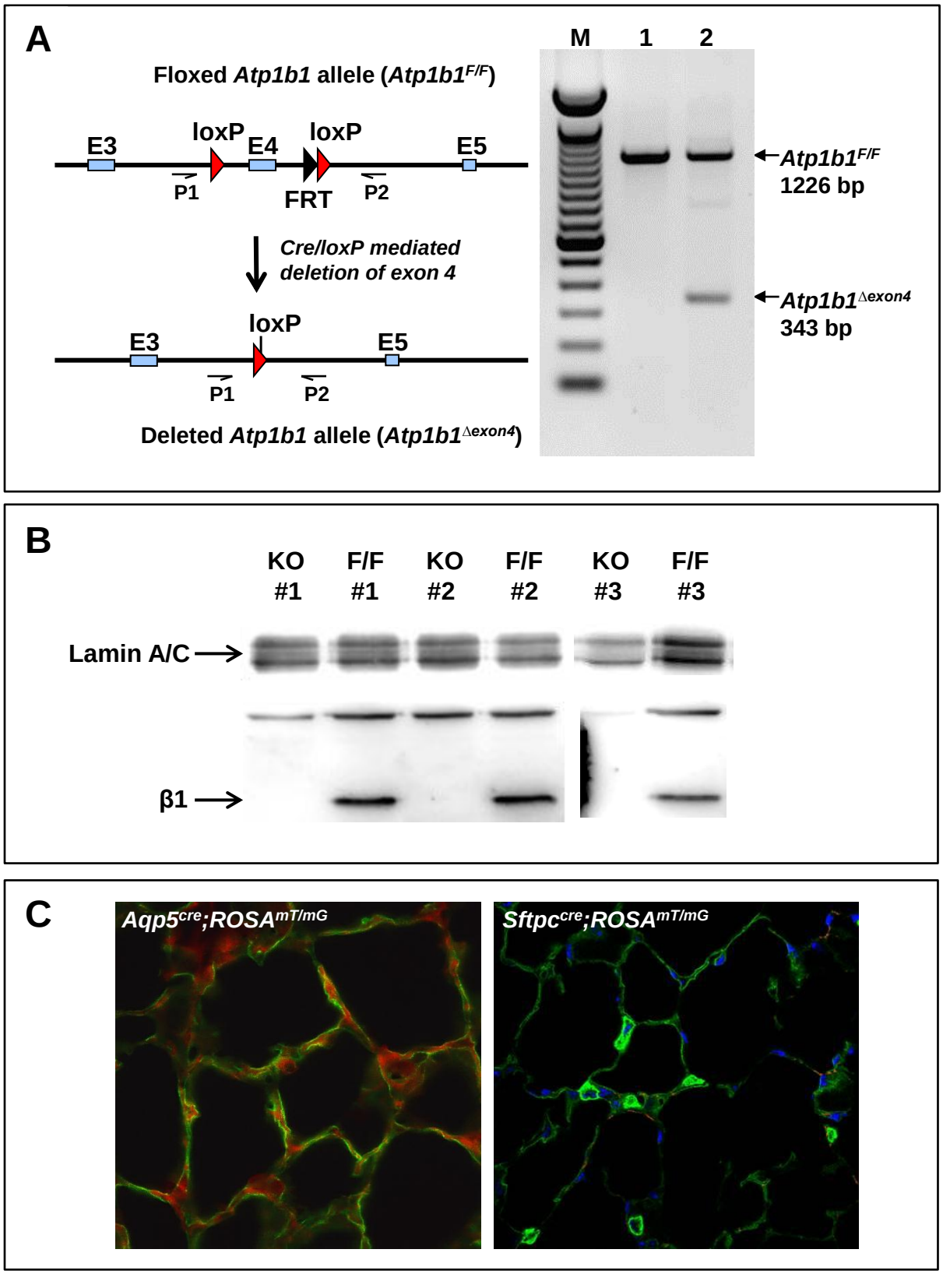

AJRCMB Articles in Press. Published on 11-April-2016 as 10.1165/rcmb.2016-0005OC

Figure E2 (online supplement)

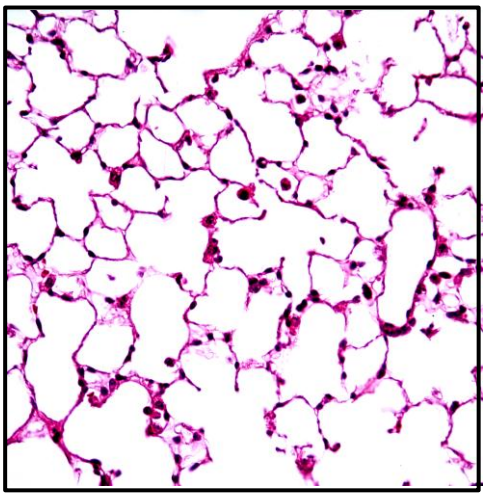

Atp1b1$^{F/F}$

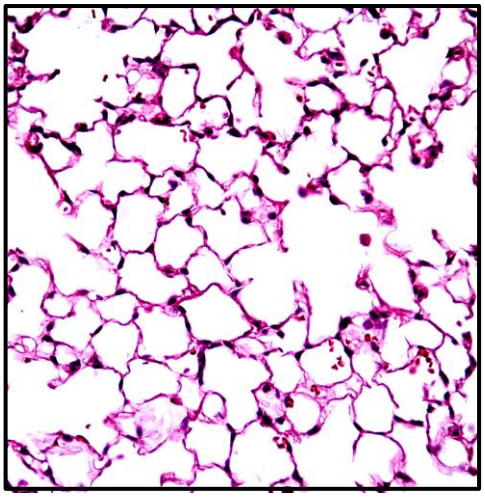

Atp1b1$^{Aqp5\text{-}cre}$

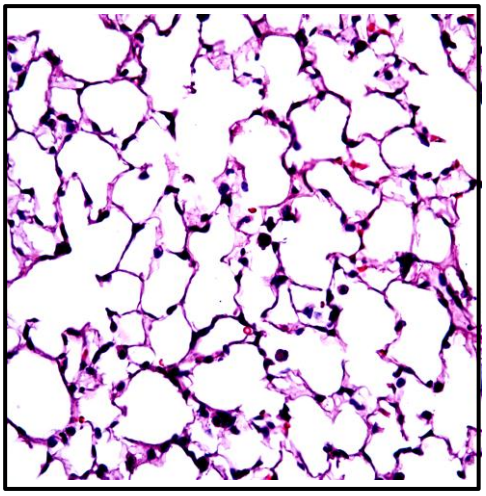

Atp1b1$^{F/F}$

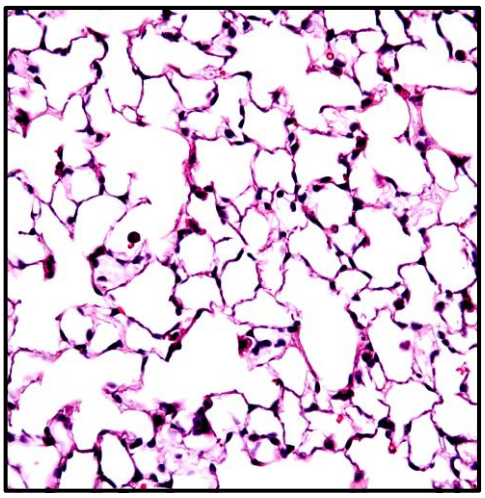

Atp1b1$^{Sftpc\text{-}cre}$